

Quantifying Intraspecific Shape Variation in the Kangaroo Humerus using Geometric Morphometrics

Thesis is presented for the Bachelor of Science in Conservation and Wild life Biology with
Honours

Environmental and Conservation Sciences
Murdoch University

Submitted by Nicole Erin Miglori

2015

Bachelor of Forensic Science (Forensic Biology and Toxicology) Bachelor of Science (Molecular
Biology and Biomedical Science) Murdoch University

Declaration

I declare this thesis is my own account of my research and contains, as its main content, work that has not been previously submitted for a degree at any tertiary education institution.

Nicole Erin Miglori (2015)

Abstract

Kangaroos exhibit one of the largest variations in body size for any vertebrate, with males being 1.5 times larger in body mass compared to females. Therefore it is assumed that sexual selection plays a major role in the behavioural and physical characteristics of kangaroos. Male and female kangaroos demonstrate marked differences in musculature of the forelimb. I investigated if the humerus (the upper bone of the forearm) of the western grey kangaroo (*Marcopus fuliginosus*) displays sexual dimorphic characteristics, and if these characteristics are correlated with muscle mass. 28 landmarks were digitised in 72 male and 23 female humeri and analysed using geometric morphometric approaches. Muscles were collected from fine dissection and residual muscle masses were calculated for analyses of each sex. Males and females were sexually dimorphic in shape, with the most obvious change at the deltoid crest where the crest was significantly increased in size and the shaft was in a bent orientation. This study suggests that a humerus from a western grey kangaroo can be classified by correct sex 92% of the time. There was a significant relationship between muscle mass and bone shape that indicate that muscles affect the morphology of the humerus. Male humeri are robust and slightly bent, conversely female obtain a more gracile form. Geometrics morphometrics is an advantageous technique that allows the morphology of shape to be investigated; by including fine muscle dissection we have determined how shape and muscles influence one another. The methods in this study can be applied to multiple studies that wish to investigate the morphology of shape and the influence of muscles.

Table of Contents

Declaration	i
Abstract.....	ii
List of figures.....	iv
List of tables	vi
Acknowledgments	vii
Chapter One:General Introduction	1
1.1 Sexual selection	1
1.2 Pre-copulatory sexual selection	2
1.2.1 Female choice.....	2
1.2.2 Male-male competition	4
1.2.3 Sexual coercion.....	4
1.3 Sexual dimorphism	5
1.4 Anatomy of the humerus	6
1.5 Sexual selection and dimorphism in the western grey kangaroo.....	11
1.6 Geometric morphometrics.....	13
1.7 General aims.....	14
Chapter Two: Methods and Materials.....	15
2.1 Data acquisition.....	15
2.1.1 Bone data	15
2.1.2 Shape analysis.....	17
2.1.3 Correlations of bone shape	18
2.1.4 Precision of measurement.....	19
Chapter Three: Results	20
3.1 What is the shape variation in the humerus?	20
Combined-sex dataset	22
How does shape variation reflect muscle development?.....	29
Chapter Four : Discussion	56
4.1 Humeral shape in kangaroos: allometric effects.....	56
4.2 Bone shape related to muscularity	58
4.3 Can we predict sex of individual from humeral shape?	60
4.4 Limitations and future research.....	62
Chapter Five: Conclusions	63
References	65
7 Appendices.....	69

List of figures

Figure 1.1 Labelled diagram, of a western grey kangaroo (<i>Macropus fuliginosus</i>) humerus. Posterior (right) and anterior (left) views. The anterior and posterior view is different due to different articulating surfaces with other bones and the muscles, which attach to them.....	7
Figure 1.2 Pictorial representation of muscle origins and insertions on the humerus of <i>M. eugenii</i> . ANL, <i>M. anconeus lateralis</i> ; ANM, <i>M. anconeus medialis</i> ; BBR, <i>M. biceps brachii</i> ; BRA, <i>M. brachialis</i> ; BRR, <i>M. brachioradialis</i> ; CBR, <i>M. coracobrachialis</i> ; ECRb, <i>M. extensor carpi radialis brevis</i> ; ECRL, <i>M. extensor carpi radialis longus</i> ; ECU, <i>M. extensor carpi ulnaris</i> ; EDC, <i>M. extensor digitorum communis</i> ; EDL, <i>M. extensor digitorum lateralis</i> ; DAC, <i>M. deltoideus pars acromialis</i> ; DCL, <i>M. deltoideus pars clavicularis</i> ; DSvC, <i>M. deltoideus pars scapularis</i> ; FCR, <i>M. flexor carpi radialis</i> ; FCU, <i>M. flexor carpi ulnaris</i> ; FDP, <i>M. flexor digitorum profundus</i> ; INF, <i>M. infraspinatus</i> ; LAT, <i>M. latissimus dorsi</i> ; PEM, <i>M. pectoralis minor</i> ; PEQ, <i>M. pectoralis quartus</i> ; PEPd, <i>M. pectoralis profundus</i> (deep); PEPs, <i>M. pectoralis profundus</i> (superficial); PAL, <i>M. palmaris longus</i> ; PRT, <i>M. pronator teres</i> ; TMA, <i>M. teres major</i> ; TMI, <i>M. teres minor</i> ; TBM, <i>M. triceps brachii caput mediale</i> ; TBLa, <i>M. triceps brachii caput laterale</i> ; SUB, <i>M. subscapularis</i> ; SPS, <i>M. supraspinatus</i> . Image and annotation from (Harvey <i>et al.</i> 2010).....	8
Figure 1.3 Male (left) and female (right) western grey kangaroos showing vast differences in size dimorphism, with the male extensively larger than the female. Image from http://www.kangaroosatrisk.net/4-how-many-kangaroos.html	12
Figure 2.1 Humeral landmarks used for geometric morphometric analysis. A) lateral, B) anterior and C) medial views of a <i>M. fuliginosus</i> humeri. Landmarks are defined in Table 2.1. Note not all landmarks are visible in each aspect	17
Figure 2.2 Scree graphs indicating relevant PCs for (a) the combined-sex dataset, (b) the male-only dataset, and (c) the female-only dataset. Scree plots of the Eigenvalues (Rip 2008) are plotted in descending order to form a curve in which an ‘elbow’ or flattening of the curve provides an indication of the number of PC factors that should be analysed.....	21
Figure 3.1. Scatter plot of Procrustes shape data PC scores for the combined-sex dataset for PC2 (y-axis) on PC1 (x-axis). Shaded diamonds represents females; males are represented by open squares. Circle is drawn around the female group to show distribution. Wireframe shows expected shape at each extremity (-0.05 for left and 0.06 for right).....	24
Figure 3.2. Correlation between centroid size and PC1 for males and females.	24
Figure 3.3. Two-dimensional scatter plot of PC1 (y-axis) on PC2 (x-axis). Shaded diamonds represents females; males are represented by open squares. Circle is drawn around the female group to show distribution. Wireframe shows expected shape at each extremity (left -0.05, right 0.05).	25
Figure 3.4 Two –dimensional scatter plot of PC3(x-axis) on PC1(y -xis), humeral Procrustes shape data. Shaded diamonds represents females; males are represented by open squares. Circle is drawn around the female group to show distribution. Wireframe shows expected shape at each extremity (left -0.04 right 0.04)	26
Figure 3.5. Two –dimensional scatter plot of PC4(x-axis) on PC1(y-axis), humeral Procrustes shape data. Shaded diamonds represents females; males are represented by open squares. Circle is drawn around the female group to show distribution. Wireframe shows expected shape at each extremity (left -0.04, right 0.03).	27
Figure 3.6. Two –dimensional scatter plot of PC5 (x axis) on PC1 (y-axis), humeral Procrustes shape data. Shaded diamonds represents females; males are represented by open squares. Circle is drawn around the female group to show distribution. Wireframe shows expected shape at each extremity(left -0.03, right 0.03).	29

Figure 3.7. Two –dimensional scatter plot of PC2 on PC1, humeral Procrustes shape data., Males are represented by open squares.....	31
Figure 3.8 Centroid size correlated with PC1 for males.	31
Figure 3.9. Two –dimensional scatter plot of PC1 on PC2, humeral Procrustes shape data. Males are represented by open squares. Wireframe shows expected shape at each extremity (left 0.05, right 0.05)	33
Figure 3.10. Two wireframes of a hypothetical humerus characterised by low PC (-0.05) and high PC (0.05) for PC2 and correlated muscles males only.	34
Figure 3.11. Two –dimensional scatter plot of PC3 on PC1, humeral Procrustes shape data. Males are represented by open squares. Wireframe shows expected shape at each extremity (left 0.03, right 0.03).	35
Figure 3.12. Two –dimensional scatter plot of PC4 on PC1, humeral Procrustes shape data., Males are represented by open squares. Wireframe shows expected shape at each extremity (left -0.04, right 0.03).....	36
Figure 3.13. Two –dimensional scatter plot of PC5 on PC1, humeral Procrustes shape data., Males are represented by open squares. Wireframe shows expected shape at each extremity(left -0.04, right 0.03).....	38
Figure 3.14. Two wireframes of a hypothetical humerus characterised by low PC (-0.04) and high PC (0.03) for PC5 and correlated muscles males only.	38
Figure 3.15. Two –dimensional scatter plot of PC2 on PC1, humeral Procrustes shape data. Females represented by shaded diamonds. Wireframe shows expected shape at each extremity (left -0.04, right 0.04).	40
Figure 3.16. Two –dimensional scatter plot of PC1 on PC2, humeral Procrustes shape data. Females represented by shaded diamonds. Wireframe shows expected shape at each extremity (left -0.03, right 0.04).	42
Figure 3.17: Centroid size correlated to PC2 for females.....	43
Figure 3.18. Two –dimensional scatter plot of PC3 on PC1, humeral Procrustes shape data. Females represented by shaded diamonds. Wireframe shows expected shape at each extremity (left-0.04, right 0.04).	44
Figure 3.19. Two wireframes of a hypothetical humerus characterised by low PC (-0.04) and high PC (0.04) for PC3 and correlated muscles females only.....	45
Figure 3.20. Two –dimensional scatter plot of PC4 on PC1, humeral Procrustes shape data. Females represented by shaded diamonds. Wireframe shows expected shape at each extremity (left -0.04, right 0.03).	46
Figure 3.21. Two wireframes of a hypothetical humerus characterised by low PC (-0.03) and high PC (0.03) for PC4 and correlated muscles females only.....	47
Figure 3.22. Two –dimensional scatter plot of PC4 on PC1, humeral Procrustes shape data. Females represented by shaded diamonds. Wireframe shows expected shape at each extremity (left -0.03, right 0.03)	48
Figure 3.23. Two wireframes of a hypothetical humerus characterised by low PC (-0.03) and high PC (0.03) for PC5 and correlated muscles females only.....	49
Figure 3.24. Two –dimensional scatter plot of PC6 on PC1, humeral Procrustes shape data. Females represented by shaded diamonds. Wireframe shows expected shape at each extremity (left -0.03, right 0.02).	50
Figure 3.25. Two wireframes of a hypothetical humerus characterised by low PC (-0.03) and high PC (0.02) for PC6 and correlated muscles females only.....	51
Figure 3.26 Two –dimensional scatter plot of PC7 on PC1, humeral Procrustes shape data. Females represented by shaded diamonds. Wireframe shows expected shape at each extremity (left -0.03, right 0.03).	52
Figure 3.27 Two wireframes of a hypothetical humerus characterised by low PC (-0.03) and high PC (0.03) for PC7 and correlated muscles females only.....	53
Figure 3.28 Two –dimensional scatter plot of PC8 on PC1, humeral Procrustes shape data. Females represented by shaded diamonds. Wireframe shows expected shape at each extremity (left -0.03, right 0.03).	54
Figure 3.29. Two wireframes of a hypothetical humerus characterised by low PC (-0.03) and high PC (0.03) for PC8 and correlated muscles females only.....	55

List of tables

Table 1.1. The muscles associated with the function of the forelimb (Hopwood 1974, Warburton, Harvey <i>et al.</i> 2011, Warburton, Bateman <i>et al.</i> 2013).....	10
Table 2.1 Humeral landmarks used for analysis (Kranioti <i>et al</i> 2009, Vance <i>et al</i> 2013).....	16
Table 3.1. Numbers of PC factor scores for each of the three datasets according to two of Joliffe's cut off value guidelines (Rip 2008).	20
Table 3.2 PC factor scores for the combined-sex dataset. The middle columns indicate which muscles were correlated with each PC factor score (Pearson's correlation coefficient; r^2) and the results for the test of sex differences in these PC factors (ANCOVA, taking body mass into account as a covariate). Statistical significance denoted by asterisks ns not significant, * $p < 0.05$, ** $p < 0.01$, *** $p < 0.001$	22
Table 3.3. Shape changes for PC1.	23
Table 3.4. Shape changes for PC2.	25
Table 3.5. Shape changes for PC3.	26
Table 3.6. Shape changes for PC4.	27
Table 3.7. Shape changes for PC5	28
Table 3.8 Muscle correlations for males.....	30
Table 3.9. Shape changes for PC1	30
Table 3.10. Shape changes for PC2	33
Table 3.11. Shape changes for PC3	35
Table 3.12. Shape changes for PC4.....	37
Table 3.13. Shape changes for PC5	37
Table 3.14 Correlated Muscles and PC scores for females	39
Table 3.15. Shape changes for PC1	40
Table 3.16. Shape changes for PC2.....	41
Table 3.17. Shape changes for PC3	44
Table 3.18. Shape changes for PC4.....	46
Table 3.19. Shape changes for PC5.....	48
Table 3.20. Shape changes for PC6.....	50
Table 3.21. Shape changes for PC7.....	52
Table 3.22. Shape changes for PC8.....	54

Acknowledgments

To all those to have helped me through this year, I thank you. I though would like to make some special thankyous to those who have been pivotal in my completion of this thesis. I would firstly like to thank my parents and family for their support through this tough year and the guidance they have given me. Especially to my mum, who has edited and read countless copies of this thesis. To James for being there at every turn. For being my shoulder to cry on when things didn't go right, to making me laugh when I needed it and for just being my Snuffy. To the anatomy staff for helping me with all my computer troubles and being kind friendly faces to talk to and being patient with me always asking for keys to the bone room and swipe cards into vet. To Sierra in radiology for taking time out of her day to process my CT scans. To Di, and Nat for helping me with my literature review. To Bec for helping me set up my Morphologika file. To my friends for allowing me to skip functions and the lack of dessert making this year so I could complete this. To Shaun for coming to Uni to have coffee, so I didn't have to leave. To my best friend Renee for allowing me to escape Uni and for being there no matter what. To my friends in the Dungeon and the Bat cave, thankyou. There are no words to describe how helpful you have all been and the support you have all given me. It was lovely knowing I could walk into any office and find friendly faces that were there to help. You are all wonderful people to whom I hope to work with in the future. Most of all thankyou to my supervisors

Natalie, Trish and Bill for giving me the opportunity to undertake this honours year. For countless meetings and hours you have invested in me. For the painful nights editing my work. For the time to help research my experiment, gaining funding and working out the faults in my digitiser. For helping me when times were tough and I was uncertain. There are so many things you have all taught me this year, that will stick with me throughout my career and there are too many words to use to thankyou.

Some dream of success while others wake up and work for it.

Chapter One:

General Introduction

1.1 Sexual selection

Darwin defined sexual selection as “*The advantage, which certain individuals have over other individuals of the same sex and species solely in respect of reproduction (pg. 256)*”. Sexual selection is driven by competition for mates. Under normal conditions in mammal populations, females are the more discerning sex, while males are more competitive for access to receptive females, this is due to parental investment in offspring. Under certain circumstances, this general pattern can be switched, e.g. due to the proportion of males in a population (Andersson *et al.* 1996, Clutton-Brock *et al.* 2009, Hosken *et al.* 2011). Sexual selection acts through both pre-copulatory strategies (female choice or female coercion) and post-copulatory strategies (including sperm competition) (Clutton-Brock *et al.* 1995).

Sexual selection occurs when differences in mating success are associated with the phenotypic deviation among individuals (Trivers 1972, Isaac 2005). Many species of mammals, such as kangaroos (Rubenstein *et al.* 1986) have a polygamous mating system in which males compete for access to females and multiple matings occur. Post-copulatory strategies are necessary for animals that have a polyandry mating system, where females mate with multiple males (Simmons 2005). Sperm competition is the main post-copulatory strategy. This is, however, out of the hands of the male, although there are ways for the male to ensure the female sire his young. An example of this is kangaroos, where the male mates multiple times

with the females and forms a copulatory plug that hypothetically prevents other males from impregnating the female (Rodger *et al.* 1975, Birkhead *et al.* 1998).

Animals of many taxa display a variety of different anatomical and physiological differences between sexes. Characteristic differences between males and females often reflect their differing roles in relation to the production and rearing of offspring (Hood 2000, Isaac 2005). In many species, females typically contribute more resources in supporting the development and rearing of young and (usually) do not heavily invest in faster growth rates or increased body size (Isaac 2005, McPherson *et al.* 2012). Males produce vast quantities of very small gametes, and are theoretically less reproductively successful compared to females; this means they have less potential to father offspring. Males therefore need to invest in secondary sexual characteristics such as size dimorphism to attract females (McCracken *et al.* 2000, McPherson *et al.* 2012, De Lisle *et al.* 2013) or in producing high quality sperm.

1.2 Pre-copulatory sexual selection

1.2.1 Female choice

Female choice is when a female chooses a male based on the characteristics or behaviours that a potential mate displays. Female choice may be influenced by a variety of factors including maturity, dominance, fertility, male investment in weaponry, symmetry, vocal and olfactory displays, genetic compatibility, and previous mating success (Clutton-Brock *et al.* 2009). Rather than a complete list,

only a selection of these factors will be examined as they relate to mammals, these examples include maturity and previous mating success.

In mammals, females are likely to choose more mature males, due to their increased size, strength and/or fertility (Miller *et al.* 2010). Females often avoid mating with immature males as they have decreased ability to be an effective defender against rival males or predatory animals (Isaac 2005, Clutton-Brock *et al.* 2009). A more mature or dominant male will actively listen to the calls of females being pressured by undesirable males, and actively try and displace them (Clutton-Brock *et al.* 2009).

In mammals, males use olfactory signalling to indicate to females that they have previously mated. By mating with previously successful males, females can gain benefits for their offspring (Clutton-Brock *et al.* 2009, Hosken *et al.* 2011). For example, the already mated male has demonstrated to the female, reproductive success and therefore fitness which will be passed on to the offspring, these are highly desirable traits (Clutton-Brock *et al.* 2009). Olfactory signalling of the recent mating, was successfully demonstrated in mice, by having a recently mated mouse and oestrus female mice in the same vicinity, female mice chose the recently-mated male over the less-recently mated male 69% of the time (Galef *et al.* 2008). Without the olfactory cue, females could not distinguish between the two sets of males and thus copulated with both groups at an equal rate (Galef *et al.* 2008).

1.2.2 Male-male competition

Male-male competition involves the competition of males for access to females (Hosken *et al.* 2011). Male dominance is asserted if the individual is larger and more robust in comparison to other males (Clutton-Brock *et al.* 2009). Male mammals possess a variety of different types of weaponry to defend, exhibit dominance or to be used in mating rituals. Males with a larger body size are more likely to gain females, and variation in size of weaponry (e.g. horns and antlers) in ungulates is strongly correlated with mating success (Bonduriansky 2007, Clutton-Brock *et al.* 2009, Warburton *et al.* 2013). For example, male moose that have larger antler and body size are more likely to attain a female due to their ability to dominate a smaller male (McPherson *et al.* 2012), while male western grey kangaroos (*Macropus fuliginosus*) use their forearms and legs in mating rituals to exhibit dominance (Grigg *et al.* 1989).

1.2.3 Sexual coercion

Sexual coercion is linked to female choice because the discerning female may not want to mate with the perusing male. Sexual coercion is any act of force or pressure that a male uses in order to copulate with a female (Clutton-Brock *et al.* 1995). There are three main types of sexual coercion that a male may use in order to copulate with a female: forced copulation, harassment, and intimidation. Forced copulation is when males use excessive speed or strength to catch, and thus physically restrain a female so he can forcefully copulate with her (Clutton-Brock *et al.* 1995). An example of this is in poeciliid fish, where the male forcefully copulates with the female by thrusting the intromittent organ into the females genital pore while the female is unaware of what is occurring (Bisazza *et al.* 2001).

Males use harassment as a tool to weaken the female by multiple attempts of copulation. This persistence comes at a cost to the female and in some cases causes her to mate immediately (Clutton-Brock *et al.* 1995). An example of this is the Japanese macaques where males are seen to follow females for up to seven days to prevent the female mating with other males and so that the female has no alternative than to mate with him (Soltistis *et al.* 1997). Intimidation is when the male uses his strength to punish a female who refuses to mate with him. This punishment acts as a physiological mechanism in which the female at some stage in the future will mate with the male to avoid physical punishment (Clutton-Brock *et al.* 1995). An example of this is bottlenose dolphins where teeth rake marks are predominately seen on oestrus females, the males use their teeth to obtain access to the females through aggressive sexual encounters (Scott *et al.* 2005).

1.3 Sexual dimorphism

Morphological, genetic and behavioural characteristic differences between males and females are referred to as sexual dimorphism, and in some instances reflect some of the most lavish and extreme examples of intraspecific variation; for example the peacock's tail or the enormous size differences between male and female elephant seals (Isaac 2005). Sexual dimorphism can be defined as the differences of traits, size or shape between males and females of the same species (Lammers *et al.* 2001). Sexual dimorphism is present in many organisms from vascular plants to invertebrates (Hood 2000). Sexual dimorphism occurs as a result of sexual selection where there are differential selective pressures acting on males and females (Soulsbury *et al.* 2014, Richards *et al.* 2015).

Rensch's Rule states that the extent of sexual size dimorphism escalates with overall body size in taxa where males are the larger of the two sexes (Rensch 1959, Hood 2000). Rensch's Rule is exhibited in many mammals and birds (Abouheif *et al.* 1997). Although Rensch's Rule is supported by male-biased sexual dimorphism, it is not the only characteristic that defines differences between males and females, any characteristic, which is different between males and females, is sexual dimorphism. For example the additional amount of body fat of female humans (Miller *et al.* 1990).

1.4 Anatomy of the humerus

The humerus is a long bone in the upper arm (brachium) (Figure 1.2). A large convex humeral head marks the proximal end, which articulates with the glenoid cavity of the scapula (Figure 1.2). Two enlarged tubercles reflect the insertion of the muscles of the rotator cuff of the shoulder (*m. supraspinatus*, *m. infraspinatus*, *m. subscapularis*, *m. teres minor*). An inter-tubercular sulcus passing between the tubercles on the anterior aspect of the bone provides a groove for the passage of the tendon of the *m. biceps brachii*. The anatomical neck lies round the head of the humerus while the surgical neck lies below the greater and lesser tubercles (Marieb *et al.* 2010). The distal epiphysis consists of two articular surfaces and an expanded surface that enables muscle attachment. The capitulum, located on the lateral surface of the condyle, articulates with the radius. The anterior aspect of the condyle is composed of a radial and coronoid fossa, which is placed proximally from the trochlea. The medial and lateral epicondyles are expansions of bone

positioned on either side of the articular condyle that function primarily for muscle attachment. The posterior surface is composed of the olecranon fossa. The fossa is an indentation that allows the olecranon of the ulna to articulate with the humerus, so movement of the lower forearm is possible. The proximal shaft of the bone often has distinctive muscle marks; the deltoid tubercle/tuberosity, the medial tubercle and the pectoral crest, reflecting the insertion of the *m. deltoideus*, *m. teres major* and *m. latissimus dorsi*, and superficial pectoral muscles, respectively (Marieb and Hoehn 2010). These features are illustrated on the humerus of a tammar wallaby (*M. eugenii*), where the muscles origin and insertions are indicated (Figure 1.2).

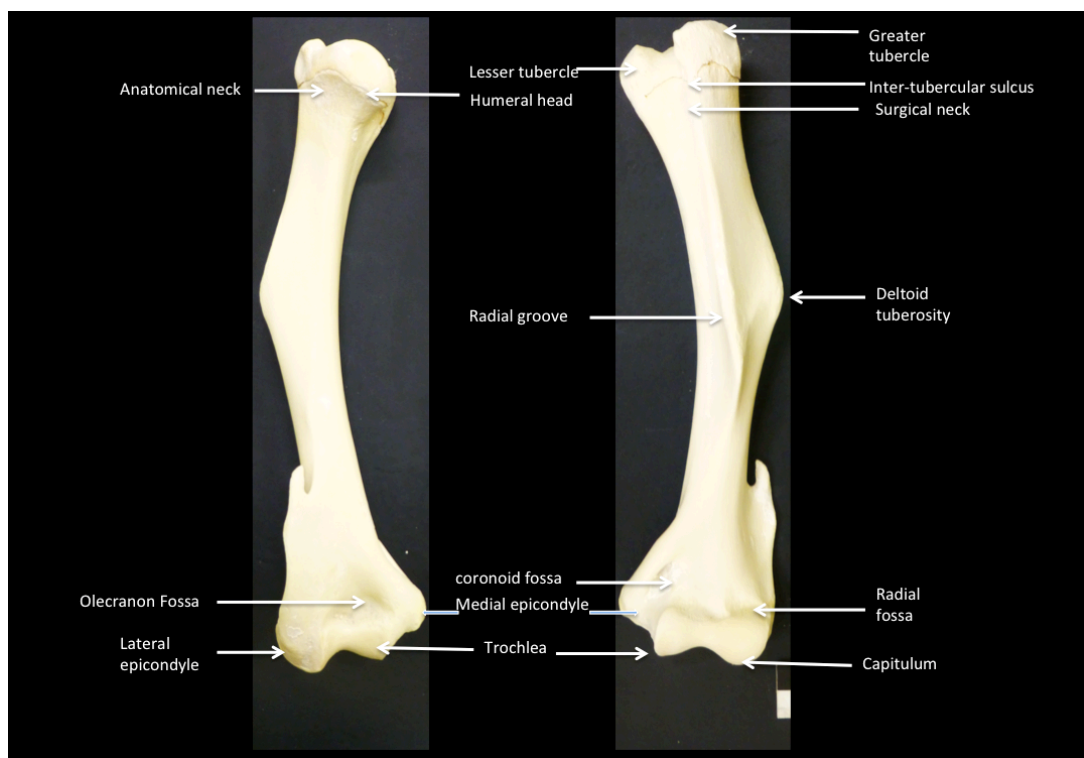


Figure 1.1 Labelled diagram, of a western grey kangaroo (*Macropus fuliginosus*) humerus. Posterior (right) and anterior (left) views. The anterior and posterior view is different due to different articulating surfaces with other bones and the muscles, which attach to them.

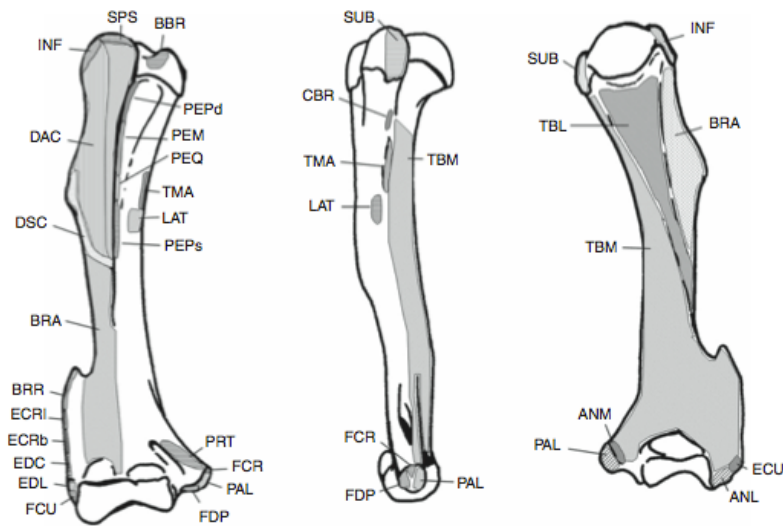


Figure 1.2 Pictorial representation of muscle origins and insertions on the humerus of *M. eugenii*. ANL, *M. anconeus lateralis*; ANM, *M. anconeus medialis*; BBR, *M. biceps brachii*; BRA, *M. brachialis*; BRR, *M. brachioradialis*; CBR, *M. coracobrachialis*; ECRb, *M. extensor carpi radialis brevis*; ECRI, *M. extensor carpi radialis longus*; ECU, *M. extensor carpi ulnaris*; EDC, *M. extensor digitorum communis*; EDL, *M. extensor digitorum lateralis*; DAC, *M. deltoideus pars acromialis*; DCL, *M. deltoideus pars claviculalis*; DSvC, *M. deltoideus pars scapularis*; FCR, *M. flexor carpi radialis*; FCU, *M. flexor carpi ulnaris*; FDP, *M. flexor digitorum profundus*; INF, *M. infraspinatus*; LAT, *M. latissimus dorsi*; PEM, *M. pectoralis minor*; PEQ, *M. pectoralis quartus*; PEPd, *M. pectoralis profundus (deep)*; PEPs, *M. pectoralis profundus (superficial)*; PAL, *M. palmaris longus*; PRT, *M. pronator teres*; TMA, *M. teres major*; TMI, *M. teres minor*; TBM, *M. triceps brachii caput mediale*; TBLa, *M. triceps brachii caput laterale*; SUB, *M. subscapularis*; SPS, *M. supraspinatus*. Image and annotation from (Harvey *et al.* 2010).

The ability for bone to functionally change to external stimuli like muscles is vital to meet the ever-changing demands of the skeleton (Sommerfeldt *et al.* 2001). When exposed to stimuli, bones can change and model and re model to suit life events. The modelling of bones occurs in the endo-cortical and periosteal surfaces of the bones and therefore has the ability to change the morphological shape for example the robustness of the medial epicondyle (Rubin 1984). The humerus, like all bones, is designed to comply with the functional demands of the animal (Sommerfeldt *et al.* 2001). The strength of these bones is accomplished by medullary space, which provide increased strength while still obtaining a minimalistic weight. This minimum weight allows the animal to be able to

accomplish tasks and movement in a energy-efficient manner (Sommerfeldt *et al.* 2001).

There are multiple stimuli that can affect the shape and structure of bones and thus affect their shape morphology, including stress levels, hormones, occupational and behavioural adaptations, and stress caused by muscles (Nigg *et al.* 2007, Currey 2014). In humans, the structural differences in the tibia of a runner and a non-runner can be visualised on the bone; the bone increases in cortical width and muscle attachments are usually more pronounced in the runner due to an increase in muscle mass applying stress to the bone (Nigg *et al.* 2007). Similarly, Cornette *et al.* (2015) showed that masseter muscles have an effect on mandible shape in shrews, they showed that an increase in muscle mass caused shape differences in the mandible specifically in the upper part of the rostrum (Cornette *et al.* 2015).

Different muscles have specific origins and insertions in the bone, which enables specific movement such as flexion and extension (Table 1.1; Figure 1.3). The amount of force a muscle applies to a bone is dependant on the functional and mechanical properties of the muscle and the mass of the muscle. When there is an absence of mechanical loading from the muscle, the bone reverts to its original genetically-determined state (Cowin 2001, Nigg *et al.* 2007). This means when the force acting upon the bone no longer exists there is no need for the bone to remodel and therefore the bone returns to its original morphology.

Table 1.1. The muscles associated with the function of the forelimb (Hopwood 1974, Harvey et al. 2011, Warburton et al. 2013)

1. Muscle	2. Function
Extrinsic muscles of the pectoral limb	
<i>Latissimus dorsi</i>	The adduction and abduction of the humerus
<i>Pectorals</i>	Adduction of humerus and forelimb
Intrinsic muscles of the pectoral limb	
<i>Deltoideus</i>	Adduction of the forelimb, involved in flexion and extension and medial to lateral rotation.
<i>Supraspinatus</i>	Abduction of the humerus. Involved in stabilisation of the shoulder joint along with M. subscapularis
<i>Infraspinatus</i>	Is associated with lateral rotation of the forelimb and shoulder stabilisation.
<i>Teres minor</i>	Apart of stabilisation and flexion of the shoulder joint
<i>Teres major</i>	Abduction and adduction of the humerus
<i>Subscapularis</i>	Adduction and medial rotation of the humerus. Contributes to shoulder stabilisation when humerus is protracted.
Muscles of the brachium	
<i>Biceps brachii</i>	Flexion of elbow
<i>Coracobrachialis</i>	Adduction of humerus
<i>Brachialis</i>	Flexion of elbow
<i>Triceps</i>	Act to extend the elbow. The extended head can also act to retraction of the humerus. In pentapedal movement the triceps maintain extension of the forelimb under the weight of the body.
<i>Tensor fascia antebrachii</i>	Works synergistically with the triceps to extend the elbow and also to tense the ante-brachial fascia
Flexors	Flexion and adduction and abduction of carpus
<i>Brachioradialis</i>	Supination of the forearm and flexion of the elbow.
Extensors	Extension and adduction.

Kangaroos use their forelimbs for a range of behaviours including feeding, grooming, fighting and for pentapedal locomotion (Hopwood *et al.* 1990). In pentapedal movement (observed in red kangaroos *M. rufus*, eastern grey kangaroos *M. giganteus*, and western grey kangaroos), the tail is counted as an accessory limb, the movement is slow and the animal visibly supports its weight on the forelimb/paws therefore providing support for the body (Hopwood *et al.*

1990). In the forward movement the weight is distributed towards the forelimb, thus creating force on those bones (Hopwood *et al.* 1990).

1.5 Sexual selection and dimorphism in the western grey kangaroo

Large macropods have large dimorphism in body size between males and females (McPherson *et al.* 2012, Rieucau *et al.* 2012, Warburton *et al.* 2013). The body size between males and females can be quite different in kangaroos (western grey kangaroo: ♂87kg, ♀ 33kg), as males can be 1.5 times heavier than females (Jarman 1989) (Figure 1.3).

Kangaroos display a polygamous mating system, which is believed to have lead to a greater degree of sexual dimorphism than monogamous mating systems (Johnson 1983). Like many mammals, kangaroos exhibit hierarchical polygamy, in which higher-ranking males have a greater opportunity compared to subordinate males. Males use their forelimbs for grappling and wrestling an opponent for female access. Male kangaroos are often involved in sparring contests in which the more dominant and males with more pronounced muscles is usually victorious due to increased strength and size (Croft *et al.* 1991). Larger male kangaroos, with greater muscle development, have more success in gaining a group of females to copulate with, compared to males with smaller musculature; thus suggesting males with larger musculature are more attractive to females (Jarman 1983, Warburton *et al.* 2013).



Figure 1.3 Male (left) and female (right) western grey kangaroos showing vast differences in size dimorphism, with the male extensively larger than the female. Image from <http://www.kangaroosatrisk.net/4-how-many-kangaroos.html>

Warburton *et al.* (2013) demonstrated differences in forelimb musculature between male and female western grey kangaroos for all forelimb muscles, where males exhibit strongly positive allometric growth and females display isometric growth. Richards *et al.* (2015) showed the length and size of the humerus is positively correlated to the length of the cranium and body size respectively in macropods, which is assumed to be a normal scaling relationship. This supports their hypothesis that the proportions of bone length in the forearm and forelimb increase under selective forces, acting on male kangaroos for stronger forelimbs thus reflecting their behaviour when it comes to female access. As external stimuli such as muscle have an influence on the morphology of bones, it is expected that there will be characteristic shape changes in the bones associated with the selection for large muscles in the forelimb of male kangaroos.

1.6 Geometric morphometrics

Shape plays a major role in biology so it is an important aspect to study. Shape is used to discriminate one organism from another, and can further discriminate tissues at a physiological level (Marcus *et al.* 2013). Traditional morphometrics, which used linear measurements, was introduced in the early 19th century, which was expanded upon by the introduction in the 1960s and 1970s of multivariate statistical tools to describe the various patterns of shape and variations within those shapes (Adams *et al.* 2004).

Geometric morphometrics (G.M.) accommodates 3D coordinates (X,Y,Z). G.M. thus has the ability to quantify shape differences between specimens, and demonstrate the use of semi-sliding landmarks (appendix 1), which can be transformed into geometrically homologous landmarks that are more helpful in the analysis of shape (Bookstein 1997, Cooke *et al.* 2015). Semi-sliding landmarks are used as they are able to show the morphological change in shape on curved surfaces while decreasing the bending energy (Adams *et al.* 2004, Zelditch *et al.* 2012).

The Procrustes method is the one of the most important parts of a G.M. analysis. The use of the Procrustes method in G.M. is due to the statistical theory of shape, derived by Kendall (Zelditch *et al.* 2012). The Generalised Procrustes Analysis (G.P.A) allows for the sample to be rotated, translated and scaled to remove information that is irrelevant to shape (Zelditch *et al.* 2012). G.M. is a method that is based on the analysis of multivariate statistical data from Cartesian coordinates, which are denoted from specific landmarks on a specimen (Slice 2007, Slice *et al.* 2009). The most common way of executing this analysis is by use of the Procrustes

method. G.M. is an advantageous technique as it has increased objectivity, applicability and repeatability (Slice 2007).

1.7 General aims

Kangaroos display one of the most extreme variations of sexual dimorphism in body weight between males and females (Miller *et al.* 2010). Due to the vast differences in sexual dimorphism there is strong evidence of sexual selection. Growth of forelimb muscles in the western grey kangaroo is different between males and females. Males exhibit larger and exaggerated muscles than females resulting from positive allometric growth. Female forelimb muscle growth occurs isometrically. No study has investigated the bones of macropods using G.M. and few have sought the link between the difference in muscle growth and bone shape.

The aims of the study are to examine the relationship between specific muscle development and the shape of the humerus in western grey kangaroos, and to compare humerus shape changes between males and females. It is predicted that increased muscularity in males will result in divergent bone morphology between the sexes, and that variation in both body size and muscularity between males may also be reflected in characteristic patterns in the bony morphology of the humerus. This study may also provide a model for future studies of limb bone shape in forensic anthropology, palaeontology, and evolutionary biology.

Chapter Two: Methods and Materials

This study examines the humeri of 95 western grey kangaroos (n=72 males, n=23 females) from the anatomy bone collection in the School of Veterinary and Life Sciences at Murdoch University. The specimens had been sourced from animals culled in the South West region of Western Australia. Previously collected associated data included: collection date and location, sex, body mass, femur circumference, individual muscle mass of intrinsic muscles of the forelimb: *m. deltoideus*; *m. supraspinatus*; *m. infraspinatus* + *m. teres minor*; *m. teres major*; *m. subscapularis*; *m. coracobrachialis*; *m. biceps brachii*; *m. brachialis*; *mm. triceps* group; grouped ante-brachial extensor and flexor muscles (Lane 2014). Humeri less than 10cm in length were considered likely to be from juvenile individual and were excluded from the investigation of humeral shape. *M. coracobrachialis* was removed from the analysis due to high variability (largely due to measurement error due to the small size of this muscle) (Warburton *et al.* 2013).

2.1 Data acquisition

2.1.1 Bone data

The data consisted of 28 humeral landmarks recorded in 3D, using a Polhemus Patriot portable digitiser running PiMgr 2.7.3 software. Landmarks were selected to correspond with known muscle attachments on the humerus and other validated landmarks from studies by Kranioti *et al.* (2009) and Vance *et al.* (2013) (Table 2.1; Figure 2.1).

Table 2.1 Humeral landmarks used for analysis (Kranioti *et al.* 2009, Vance *et al.* 2013).

Proximal epiphysis

- | | |
|----|-------------------------------------------------------------------------------|
| 1 | The point of convection of the humeral head around the base |
| 2 | The indentation between the lesser tubercle and the humeral head |
| 3 | Bottom of the lesser tubercle on the inside of the inter-tubular sulcus |
| 4 | Bottom of the greater tubercle on the inside of the inter-tubular sulcus |
| 5 | Where the line of the deltoid crest meets the epiphyseal line |
| 6 | The end of the line where the greater tubercle ends. |
| 7 | The point just after the rounding of the humeral head |
| 8 | Most superior point of the lesser tubercle |
| 9 | Point of where the lesser tubercle meets the top of the inter-tubular sulcus |
| 10 | Point of where the greater tubercle meets the top of the inter-tubular sulcus |
| 11 | Most superior part of the greater tubercle |
| 12 | Top the ear-like tubercle of the greater tubercle |

Shaft

- | | |
|----|------------------------------------------------------------------|
| 13 | Deepest point before the bone becomes rough of the deltoid crest |
| 14 | Most medial point of the deltoid crest |
| 15 | Last point of roughness on the deltoid crest |
| 16 | Point of incision between the deltoid and pectoral crest |
| 17 | Parallel line from landmark 14 |
| 18 | Tuberosity along the line stemming from the lesser tubercle. |

Distal

- | | |
|----|--------------------------------------------------------------|
| 19 | Top of the extension of the lateral epicondyle |
| 20 | Bottom of the well between the shaft and the lateral spike |
| 21 | Most lateral part of the lateral epicondyle |
| 22 | Top of the capitulum |
| 23 | Middle of trochlea (inferior aspect) |
| 24 | Top of trochlea upper left corner |
| 25 | Top of supracondyloid foramen |
| 26 | Bottom of supracondyloid foramen |
| 27 | Between the trochlea and medial epicondyle (inferior aspect) |
| 28 | Most medial aspect of medial epicondyle |

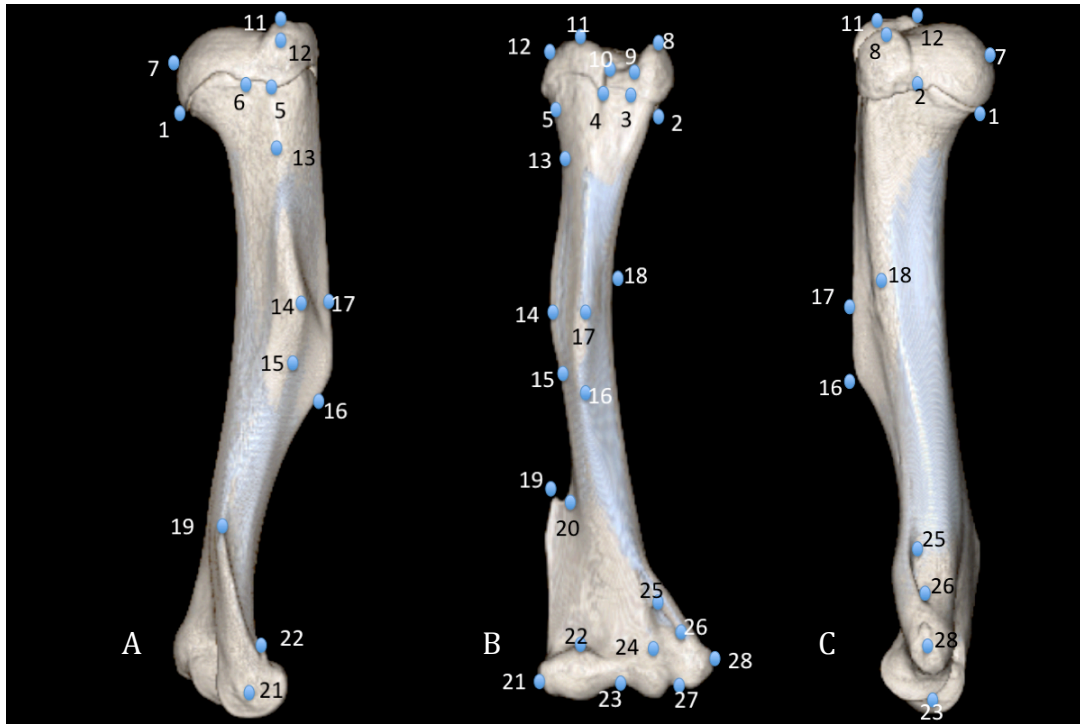


Figure 2.1 Humeral landmarks used for geometric morphometric analysis. A) lateral, B) anterior and C) medial views of a *M. fuliginosus* humeri. Landmarks are defined in Table 2.1. Note not all landmarks are visible in each aspect.

2.1.2 Shape analysis

The shape analysis software *morphologika* (www.york.ac.uk/res/fme) (O'Higgins et al. 1999) was used to analyse the three-dimensional coordinates of the landmarks. To remove non-shape variation in the sample, the raw landmark coordinates from all humeri were first transformed using a Generalised Procrustes Analysis (GPA). This involves rotating, translating and re-scaling the images relative to each other (Dryden *et al.* 1998). This process alters the landmark coordinates so that each humerus has a unit in centroid size. The scatter points for each specimen are projected from Kendall's shape space to Euclidean tangent space, which allows statistical analysis to be undertaken (O'Higgins 2000).

Principal Components Analyses (PCA) was used to examine shape variation amongst the samples for three sets of the data: males and females combined, males

only, and females only. The statistical analyses use selected scores from GPA/PCA of the sample as the number of variables is required to be less than the number of specimens (Franklin *et al.* 2007).

2.1.3 Correlations of bone shape

Multivariate regression analysis was used to test for sex differences in the sample. The dependant variable was PC scores and the independent variable was sex (Franklin *et al.* 2007). Analysis of Covariance (ANCOVA) was used to test for sexual dimorphism in humerus shape for each of the PC factor scores as the dependant variables for separate analyses, with sex as the categorical factor and the different muscles as covariates. Spearman Rank Order correlation matrix was used to quantify the relationship between the PC factor scores with centroid size. Discriminate analysis with cross validation was used to assess sex and population classification accuracy, with the dependant variable being the different PC scores and sex as the categorical factor.

To determine if muscle mass had a potential correlation to shape variation of the humerus, Spearman rank correlation output was used to indicate patterns of change. Due to sex differences in relationship with body mass for forelimb muscles (males positively allometric, females isometric), residual muscle masses were calculated for each sex separately using PAST (version 2.17). Given that there are clear differences in muscle development between males and females, each sex was analysed separately in order to better understand the relationship between bone shape and muscularity. For these analyses the residuals of the muscles masses of individuals were used as these correspond to the muscularity of the individual.

The reasoning for using absolute muscle mass for the combined analysis is that this gives a direct comparison between males and females; this will help determine the differences between males and females. Residual muscle mass is used, due to the differences within the separate groups in terms of muscularity.

Sexual difference between muscles in combined males and females was determined by an ANCOVA. This was to indicate that though the muscle is correlated with both is the muscle affecting the groups in different ways.

2.1.4 Precision of measurement

The degree of measurement error in landmark acquisition was assessed by repeated digitising of five points (landmarks 4, 17, 18, 20 and 23) of a sample bone (KML 11) every day (n=8) before analysis. Measurement error was calculated by using the Procrustes output coordinate for each landmark; the standard deviation was then calculated for each landmark by using the following equation(von Cramon-Taubadel, *et al.* 2007).

$$\sigma = \sqrt{\sum_{i=1}^N (xi - \overline{x}) + (yi - \overline{y}) + (zi - \overline{z})/3N}$$

The landmark error was then calculated (where a, b, c, d, e, are the reference landmarks)

$$\sigma = \sqrt{\sigma_a^2 + \sigma_b^2 + \sigma_c^2 + \sigma_d^2 + \sigma_e^2/5}$$

The average reference landmark error for all five landmarks was 0.09mm.

All statistical analyses were carried out using Statistica 7.1 (for windows 2007).

Chapter Three: Results

3.1 What is the shape variation in the humerus?

Joliffe's cut off value guidelines (Rip 2008) was used to determine the number of biologically important Principal Component (PC) factors. Joliffe's first rule of over 70% of the variation in each dataset and fourth rule of visual interpretation of the scree plots (Figure 2.2) were relevant to these data, but yielded slightly different results (Table 3.1). This was resolved by taking the smaller amount of PC scores due to the little variation (less than 1 %), which occurred after the PC cut off.

However this study used 8 PC scores in females due to the elbow affect not being as obvious in females as in was in the combined and male only data set. The second rule assumes that no eigenvalues will be used if they are less <1 was not applicable, as all eigenvalues were <1. Joliffe's third rule indicates that eigenvectors should be used to the 0.1 and 0.2, Joliffe indicated that this included too many eigenvectors and that 0.7 is more appropriate.

Table 3.1. Numbers of PC factor scores for each of the three datasets according to two of Joliffe's cut off value guidelines (Rip 2008).

Dataset	>70% of variation in the dataset	Visual analysis of the scree plots
1. Combined-sex dataset	10	5
2. Male-only dataset	10	5
3. Female-only dataset	7	8

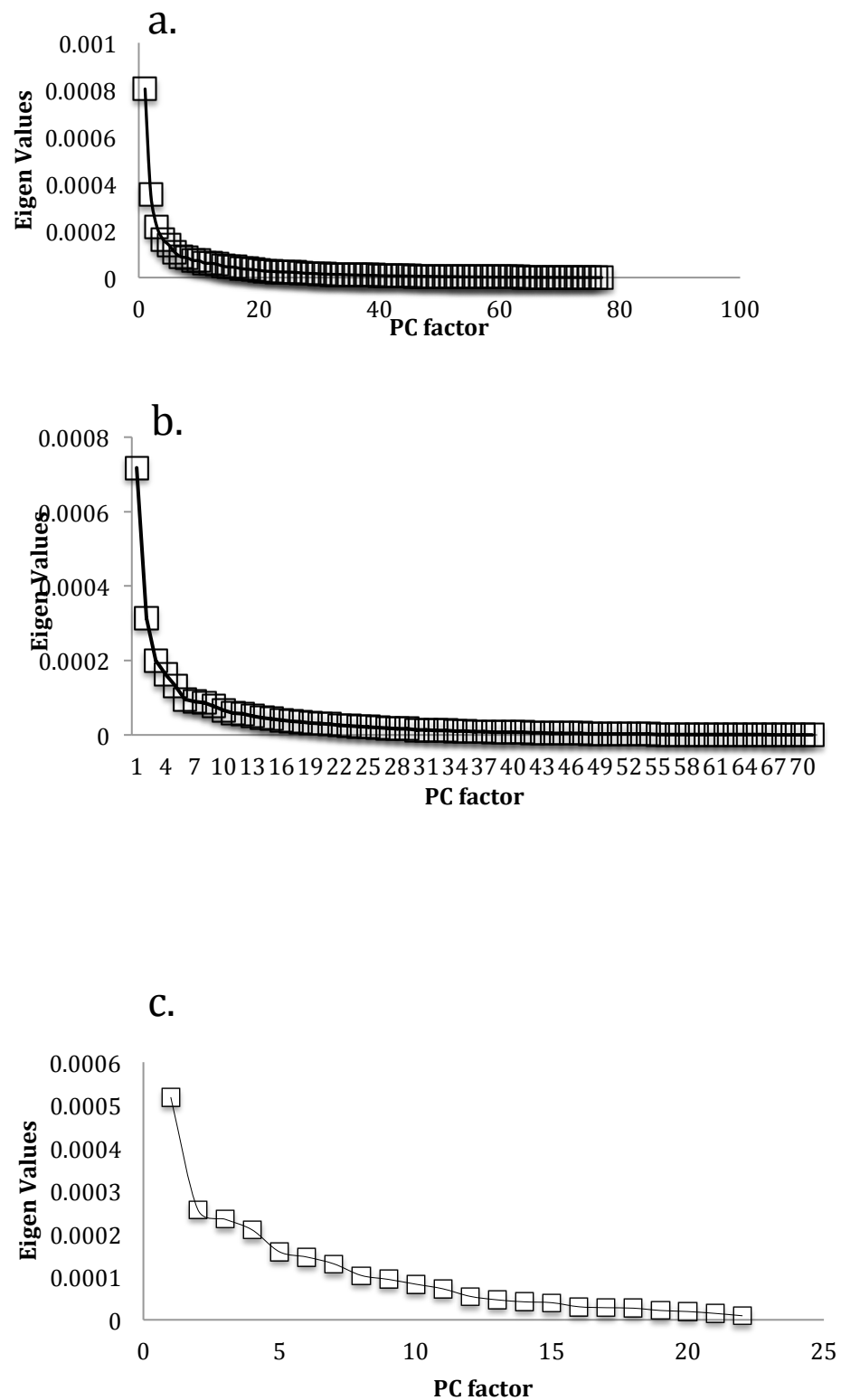


Figure 2.2 Scree graphs indicating relevant PCs for (a) the combined-sex dataset, (b) the male-only dataset, and (c) the female-only dataset. Scree plots of the Eigenvalues (Rip 2008) are plotted in descending order to form a curve in which an ‘elbow’ or flattening of the curve provides an indication of the number of PC factors that should be analysed.

Combined-sex dataset

There were five PC factor scores that described the shape data for the combined-sex dataset. Of these, there were significant sex differences only for PC1, and correlations with absolute muscle mass values only for PC1 (Table 3.2).

Table 3.2 PC factor scores for the combined-sex dataset. The middle columns indicate which muscles were correlated with each PC factor score (Pearson's correlation coefficient; r^2) and the results for the test of sex differences in these PC factors (ANCOVA, taking body mass into account as a covariate). Statistical significance denoted by asterisks ns not significant, * $p < 0.05$, ** $p < 0.01$, *** $p < 0.001$.

PC factor	% Variation	ANOVA for sex differences	Significant correlations with muscle mass (g)	r^2	Sex difference (ANCOVA)
PC1	26.9%	$F_{1, 93} = 55.09$ ***	<i>M. supraspinatus</i>	0.7719 ***	$F_{1, 92} = 11.60$ ***
			<i>M. supraspinatus</i> & <i>M. teres minor</i>	0.7520 ***	$F_{1, 92} = 13.04$ ***
			<i>M. teres major</i>	0.7288 ***	$F_{1, 92} = 13.04$ ***
			<i>M. subscapularis</i>	0.7464 ***	$F_{1, 92} = 179.17$ ***
			<i>M. biceps brachii</i>	0.7141 ***	$F_{1, 92} = 12.11$ ***
			<i>M. brachialis</i>	0.7367 ***	$F_{1, 92} = 9.98$ **
			<i>M. triceps brachii</i> & <i>M. tensor fasciae antebrachii</i>	0.7337 ***	$F_{1, 92} = 9.73$ **
			Extensors	0.7345 ***	$F_{1, 92} = 9.08$ **
			Flexors	0.7194 ***	$F_{1, 92} = 10.14$ **
			<i>M. latimus dorsi</i>	0.8578 ***	$F_{1, 92} = 2.94$, ns
			Pectoral muscles	0.7895 ***	$F_{1, 92} = 4.22$ *
PC2	11.8%	$F_{1, 93} = 4.22$ *	N		Ns
PC3	7.3%	$F_{1, 93} = 20.06$ ***	N		Ns
PC4	5.5%	$F_{1, 93} = 4.56$ *	Ns		Ns
PC5	4.6%	$F_{1, 93} = 1.66$	Ns		Ns

PC1 accounted for 26.9% of the total variance in the combined-sex dataset. The PC is characterised by changes in overall surface area of muscle attachment and changes in shape morphology (Table 3.3). There were significant sexual differences in PC factor 1 in the discriminate analysis of the combined sex dataset (Wilk's $\lambda = 0.343$, corresponding to a $F_{5, 89} = 34.109$ ***). The cross-validated discriminate analysis shows that when using PCs 1-5 overall expected accuracy is

92.6% (males 94.44% and females 86.9%). Though there is a large sex bias of 7.54%

Table 3.3. Shape changes for PC1.

Low PC score	High PC score
<ul style="list-style-type: none"> • Small humeral head and proximal tubercles • Narrow inter-tubercle sulcus • Bulbous head • Gracile shaft, low torsion • Transversely narrow distal epiphysis 	<ul style="list-style-type: none"> • Increase width and height of the greater and lesser tubercle • Increased breadth of the inter-tubercle sulcus • More flattened humeral head • Increased robustness and torsion of shaft (especially around pectoral crest) • Distal placement of lateral epicondyle • Proximal placement of landmark 27 • Medial expansion of the medial epicondyle

Females have significantly lower PC 1 scores (Figure 3.1; indicated by circle). PC1 was strongly correlated with the centroid size (appendix 1) ($p < 0.001$; Figure 3.2) and also body mass (log-transformed) ($p < 0.001$; Figure 3.3). The ANCOVA of PC1 and body mass (log-transformed) showed differences between males and females ($F_{1,90} = 42.05, p < 0.001$). The result of this analysis indicated that males and females were different in terms of body mass due to the difference in the slope between males and females. PC1 was correlated with the mass of all intrinsic muscles measured, with the exception of *m. deltoideus* (Table 3.2). ANCOVA was used to test the relationship between the bone-PC1 and muscle mass, with body mass as a covariate and sex as a categorical factor. The results show significant sex differences in the residual of PC1 with body mass. This means that once accounting for differences in gross body mass, there is still an effect of the different muscle masses on the shape of the bone and thus indicates significant sex differences (Table 3.2). The *F* statistics generated showed that each muscle had a *p* score of less than 0.05, which indicates that there is a significant difference between the male and female muscles (Table 3.2).

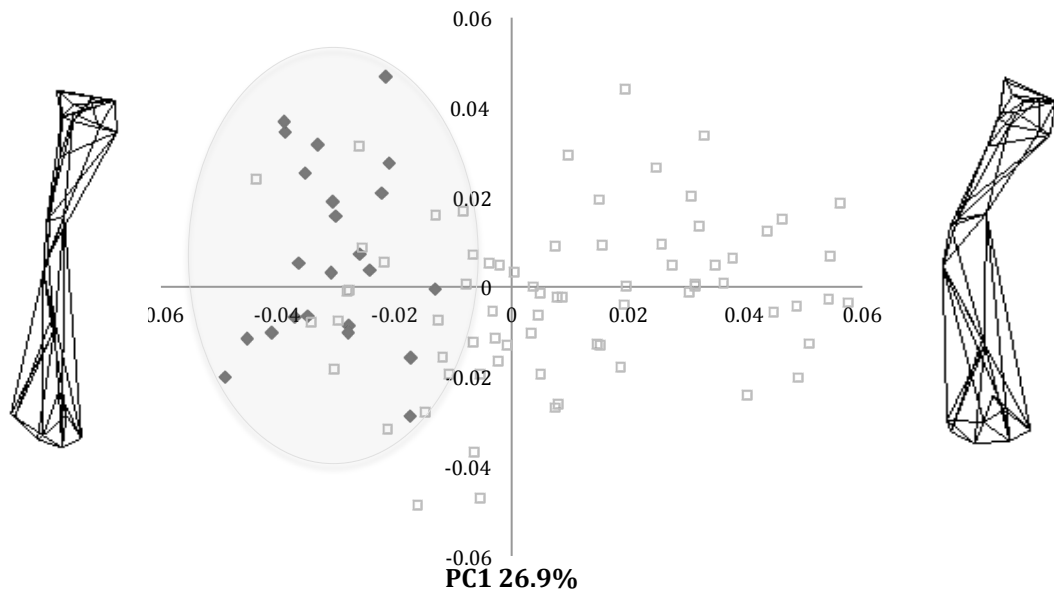


Figure 3.1. Scatter plot of Procrustes shape data PC scores for the combined-sex dataset for PC2 (y-axis) on PC1 (x-axis). Shaded diamonds represents females; males are represented by open squares. Circle is drawn around the female group to show distribution. Wireframe shows expected shape at each extremity (-0.05 for left and 0.06 for right).

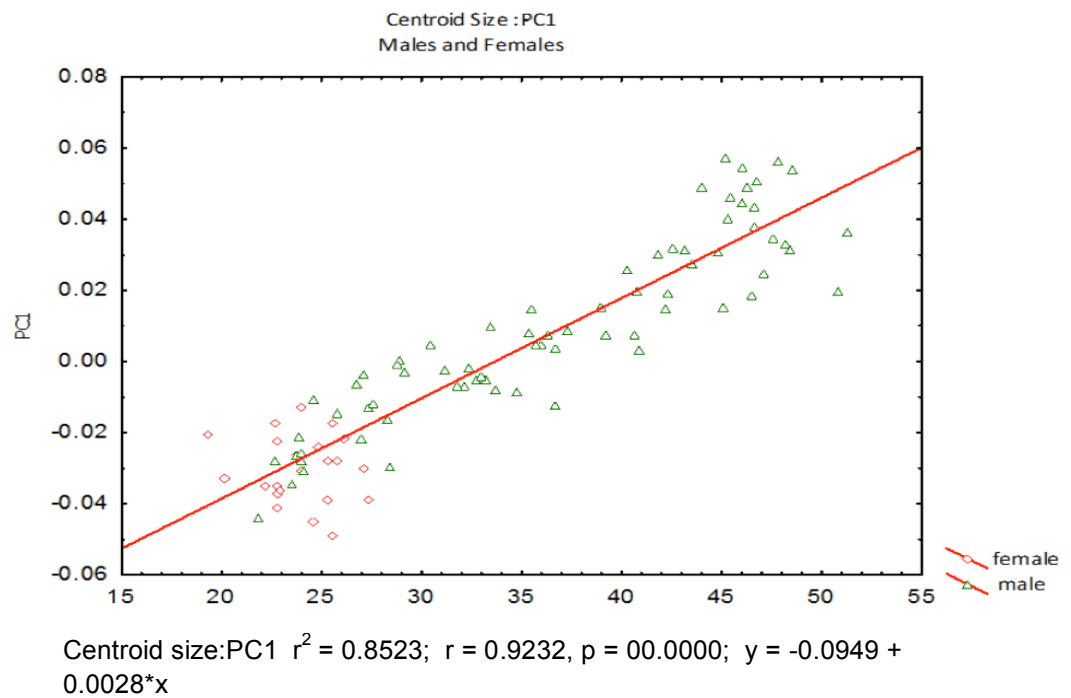


Figure 3.2. Correlation between centroid size and PC1 for males and females.

PC2 accounted for 11.8% of the total variance in the combined-sex dataset. The PC is characterised by differences in width and height of the greater and lesser

tubercles a more bulbous head protruding away from the anatomical neck, pectoral and deltoid crest along with changes in the distal epiphysis (Table 3.4; Figure 3.3).

Table 3.4. Shape changes for PC2.

Low PC	High PC
<ul style="list-style-type: none"> • Relatively narrow greater and lesser tubercles with relatively acute peaks • A less bulbous head at the level of the anatomical neck • Relatively narrow around the shaft • Distal placement of the deltoid and pectoral crests • Relatively narrow distal epiphysis 	<ul style="list-style-type: none"> • Transversely broader proximal tubercles which appeared more flattened at most proximal points • Relatively bulbous head protruding away from the anatomical neck • Increased breadth of the shaft • Proximal placement of deltoid and pectoral crest • Transversely widened distal epiphysis

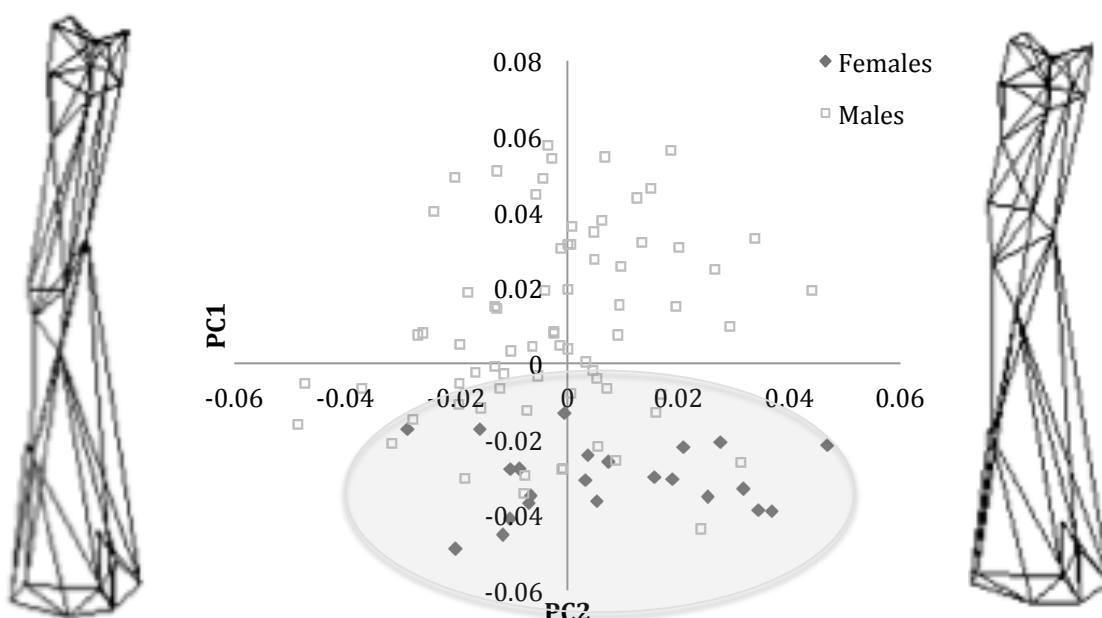


Figure 3.3. Two-dimensional scatter plot of PC1 (y-axis) on PC2 (x-axis). Shaded diamonds represents females; males are represented by open squares. Circle is drawn around the female group to show distribution. Wireframe shows expected shape at each extremity (left -0.05, right 0.05).

PC3 accounted for 7.3% of the total variation in combined-sex dataset. The PC is characterised by the changes in height and width of the greater and lesser tubercles, a more robust shaft with proximally placed deltoid and pectoral crest along with torsion of the shaft. There were also changes on the distal epiphysis.

Tubercles and humeral head, deltoid and pectoral crest along with changes in the extension of the lateral epicondyle placed distally (Table 3.5; Figure 3.4).

Table 3.5. Shape changes for PC3.

Low PC score	High PC score
<ul style="list-style-type: none"> • Relatively small humeral head and tubercles • A less bulbous head at the level of the anatomical neck • Relatively gracile and elongated shaft • Distally placed pectoral and deltoid crest • Transversely narrow distal epiphysis • Extension of lateral epicondyle placed distally 	<ul style="list-style-type: none"> • Relatively wide and flat proximal tubercles • Relatively bulbous head protruding away from the anatomical neck • Relatively robust shaft • Deltoid and pectoral crests were more proximally placed and slight torsion occurred • Transversely wider at distal epiphysis

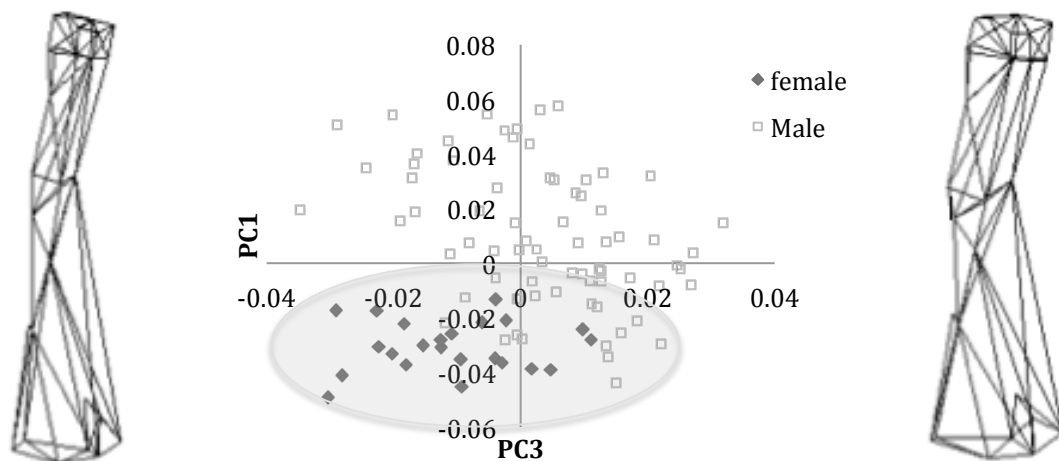


Figure 3.4 Two –dimensional scatter plot of PC3(x-axis) on PC1(y -xis), humeral Procrustes shape data. Shaded diamonds represents females; males are represented by open squares. Circle is drawn around the female group to show distribution. Wireframe shows expected shape at each extremity (left -0.04 right 0.04)

PC4 accounted for 5.5% of the total variation in the combined-sex dataset. The PC is characterised by changes in the greater tubercle, less bulbous appearance at the level of the anatomical neck, narrowing of shaft and distal epiphysis along with movement of the supracondyloid foramen and extension of the lateral epicondyle (Table 3.6; Figure 3.5).

Table 3.6. Shape changes for PC4.

Low PC score	High PC score
<ul style="list-style-type: none"> • Relatively narrow tubercles and increased in height at proximal points • Relatively bulbous head protruding away from the anatomical neck • Shaft became more robust at the top third. • Lateral placement of deltoid crest • Proximal and posterior placement of medial tuberosity • Distally placement of the extension of the lateral epicondyle and decreased in length • Relatively narrow distal epiphysis 	<ul style="list-style-type: none"> • Inferior placement and flattening of the greater tuberosity • A less bulbous head at the level of the anatomical neck • And lateral angulation of the inter-tubercle sulcus • Relatively narrow and gracile shaft, around the top third • Distal and anterior placement of the medial tuberosity • The extension of the lateral epicondyle on the distal epiphysis was proximally placed with relative increase in length • The supracondyloid foramen was more proximally located and the distal epiphysis was transversely wide

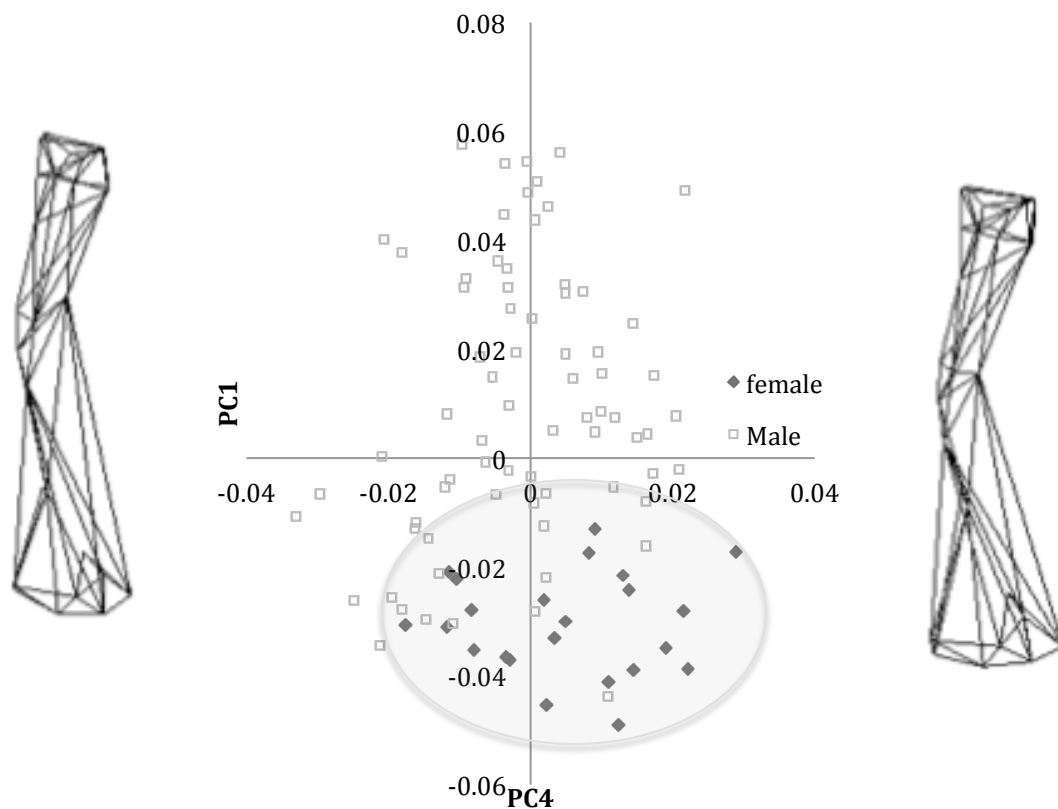


Figure 3.5. Two –dimensional scatter plot of PC4(x-axis) on PC1(y-axis), humeral Procrustes shape data. Shaded diamonds represents females; males are represented by open squares. Circle is drawn around the female group to show distribution. Wireframe shows expected shape at each extremity (left -0.04, right 0.03).

PC5 accounted for 4.6% of the total variation in the combined-sex dataset. The PC is characterised by changes in the width of the proximal epiphysis, lateral placement of greater and lesser tubercles, extreme bending of shaft along with distal placement of deltoid crest and transverse widening of the distal epiphysis (Table 3.7;Figure 3.6).

Table 3.7. Shape changes for PC5

Low PC scores	High PC scores
<ul style="list-style-type: none"> • Relative decreased head and breadth size • The tubercles placed medially, relative increase in breadth of inter-tubercle sulcus • Relatively narrow shaft and bending is observed • The most distal extremity of the deltoid crest is medially placed • The extension of the lateral epicondyle is placed in the anterior aspect • The supracondyloid foramen is proximally placed 	<ul style="list-style-type: none"> • Relative increased head and breadth size • The tubercles are placed laterally • Inter-tubercle sulcus relatively small in size • The shaft was extremely bent and widened • The distal third, of the deltoid crest is laterally placed • The extension of the lateral epicondyle is placed in the posterior aspect and the supracondyloid foramen is distally placed • Transversely wider distal epiphysis

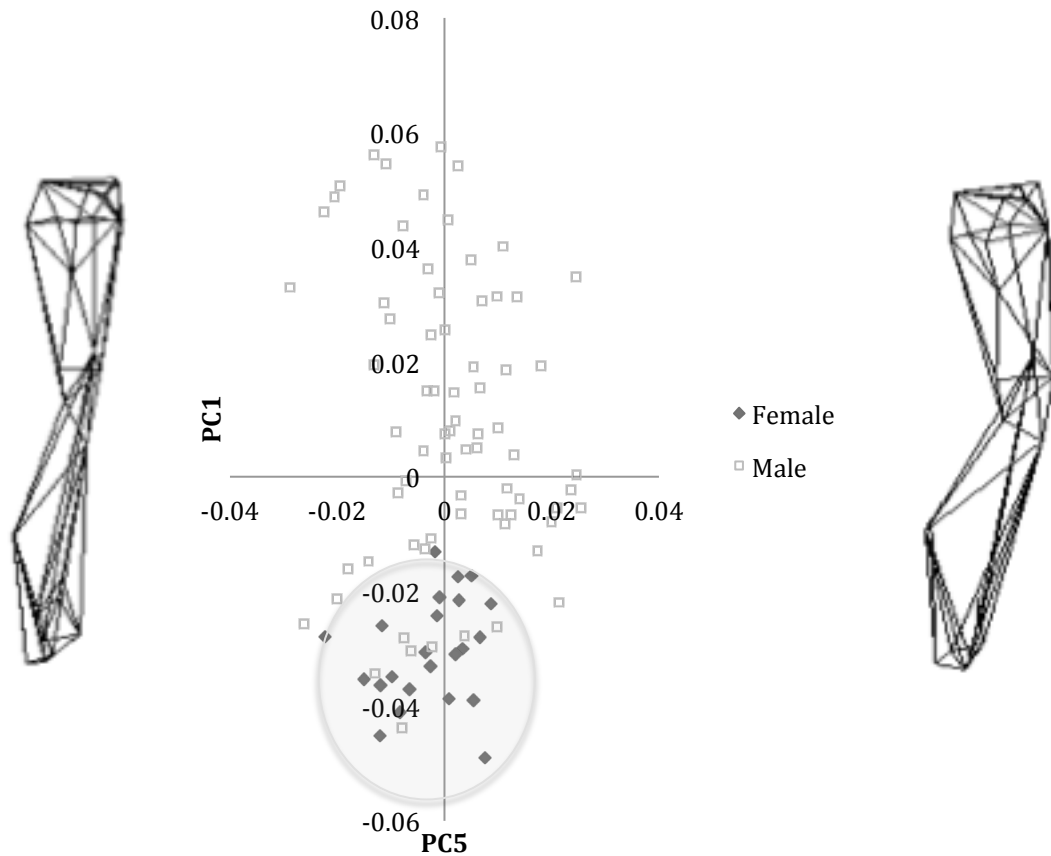


Figure 3.6. Two –dimensional scatter plot of PC5 (x axis) on PC1 (y-axis), humeral Procrustes shape data. Shaded diamonds represents females; males are represented by open squares. Circle is drawn around the female group to show distribution. Wireframe shows expected shape at each extremity(left -0.03, right 0.03).

How does shape variation reflect muscle development?

There were five PC's that described the shape data for the male-only dataset. Of these, there were significant differences in residual muscle correlations for PC2 and PC5 (Table 3.8).

Table 3.8 Muscle correlations for males.

PC	Correlated muscles /centroid
Males	
PC1 (26.1%)	Centroid r^2 0.8590 ***
PC2 (11.5%)	<i>M. Deltoideus</i> (g) r^2 0.1260 ** <i>M. Supraspinatus</i> r^2 0.0708 * <i>M. Subscapularis</i> r^2 0.0633 * <i>M. Teres major</i> r^2 0.0618 *
PC3 (7.3%)	
PC4 (5.9%)	
PC5 (4.8%)	<i>M. Supraspinatus</i> r^2 0.0551 * <i>M. Subscapularis</i> r^2 0.0534 * <i>M. Teres major</i> r^2 0.0365 Extensors r^2 0.0372

* $p < 0.05$ ** $p < 0.01$ *** $p < 0.001$

PC1 accounted for 26.1% of the total variance in the male-only data set. The PC is characterised by, changes in the greater and lesser tubercles, robustness of the shaft, and changes in the distal epiphysis (Table 3.9; Figure 3.7). There were no muscles correlated with this PC (Table 3.8). PC1 was also correlated with centroid size (Figure 3.8)($p < 0.001$).

Table 3.9. Shape changes for PC1

Left of graph	Right of Graph
<ul style="list-style-type: none"> • Tubercles increased in relative size • Relatively bulbous head protruding away from the anatomical neck • The shaft became more gracile, deltoid and pectoral crests are placed proximally • Shaft was relatively straight • The extension of the lateral epicondyle was placed in the anterior aspect • Distal and medial placement of the medial epicondyle • Lateral and proximal placement of the lateral epicondyle • Trochlea and capitulum moved further in proximity and decreased in height 	<ul style="list-style-type: none"> • Tubercles decreased in relative size • A less bulbous head at the level of the anatomical neck • The shaft became more robust with the deltoid and pectoral crests are placed proximally and bending of the shaft was obvious • The pectoral crest was placed posteriorly • The extension of the lateral epicondyle was placed in the posterior aspect • Proximal and medial placement of the medial epicondyle, distal and medial placement of the lateral epicondyle • Trochlea and capitulum moved closer in proximity and increased in height

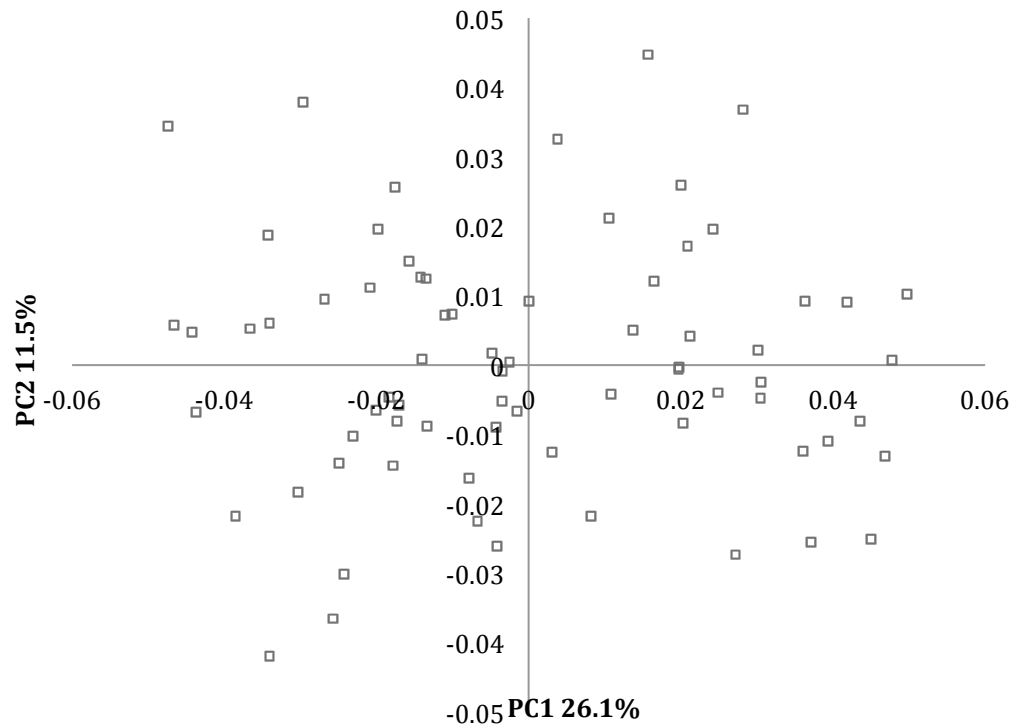
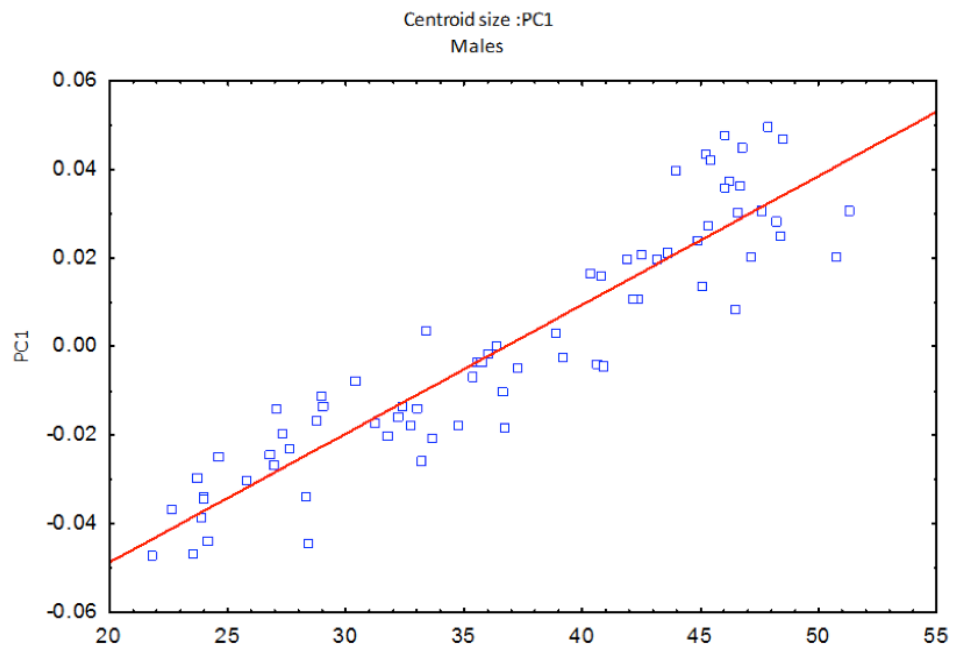


Figure 3.7. Two –dimensional scatter plot of PC2 on PC1, humeral Procrustes shape data., Males are represented by open squares.



Centroid size: PC1: $r^2=0.8590$; $r=0.9268$, $p=0.0001$; $y=0.1068+0.0029*x$

Figure 3.8 Centroid size correlated with PC1 for males.

The shape variation among the males in isolation followed very similar patterns in the first five PC axes as those described for the males and females combined (as would be expected given the disproportionately larger number of males included in the sample, and the much greater variation in size and shape amongst the sample of bones).

PC2 accounted for 11.5% of the total variance of the male-only dataset. The PC is characterised by changes in relative size of the proximal epiphysis, laterally placed pectoral crest and extension of the lateral epicondyle placed medially (Table 3.10;Figure 3.9). Males were evenly distributed over the graph for PC2: PC1. There were significant correlations with residual muscle mass values (Table 3.8;Figure 3.10)

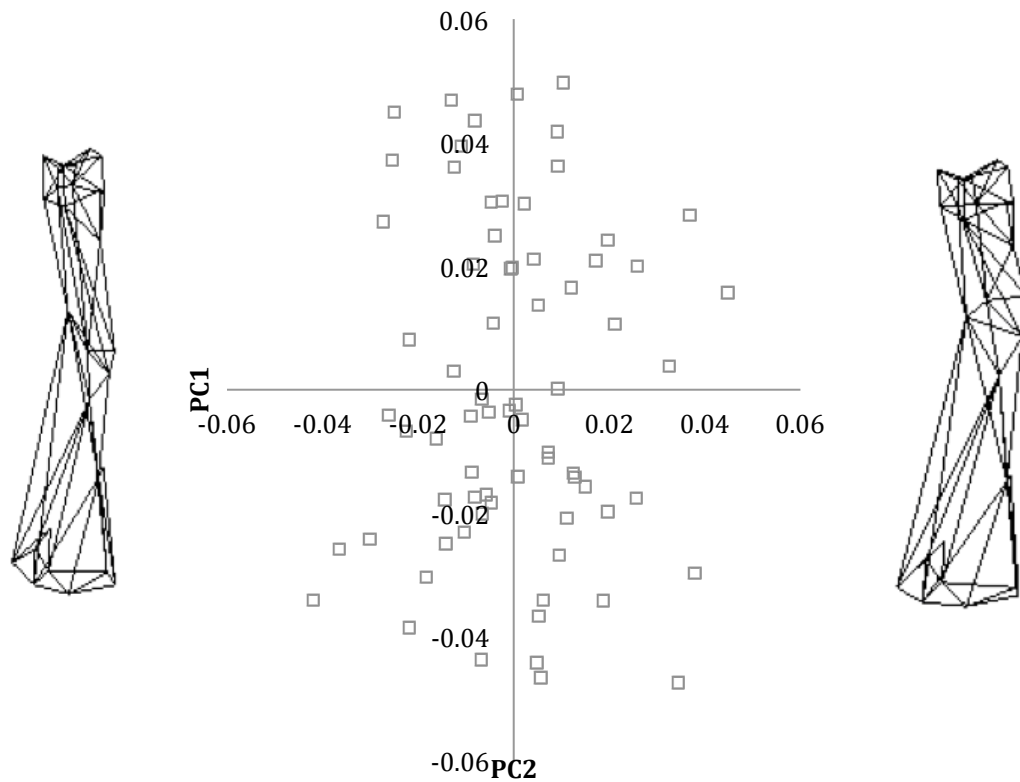


Figure 3.9. Two –dimensional scatter plot of PC1 on PC2, humeral Procrustes shape data. Males are represented by open squares. Wireframe shows expected shape at each extremity (left 0.05, right 0.05)

Table 3.10. Shape changes for PC2

Low PC score	High PC score
<ul style="list-style-type: none"> • Relative decreased size of the proximal epiphysis • Greater and lesser tubercles narrow, most proximal points became pointed • Inter-tubercle sulcus decreased in relative size • Shaft became gracile, • Pectoral and deltoid crest placed medially and distally • Decreased breadth of the distal epiphysis • Medial epicondyle placed proximally • Extension of the lateral epicondyle placed laterally 	<ul style="list-style-type: none"> • Relative increased size of the proximal epiphysis • Greater and lesser tubercles widened, most proximal points of tubercles flattened • Inter-tubercle sulcus widened • Shaft became robust. Pectoral and deltoid crest are placed proximally • Increased breadth of the distal epiphysis • Medial epicondyle placed distally • Extension of the lateral epicondyle placed medially

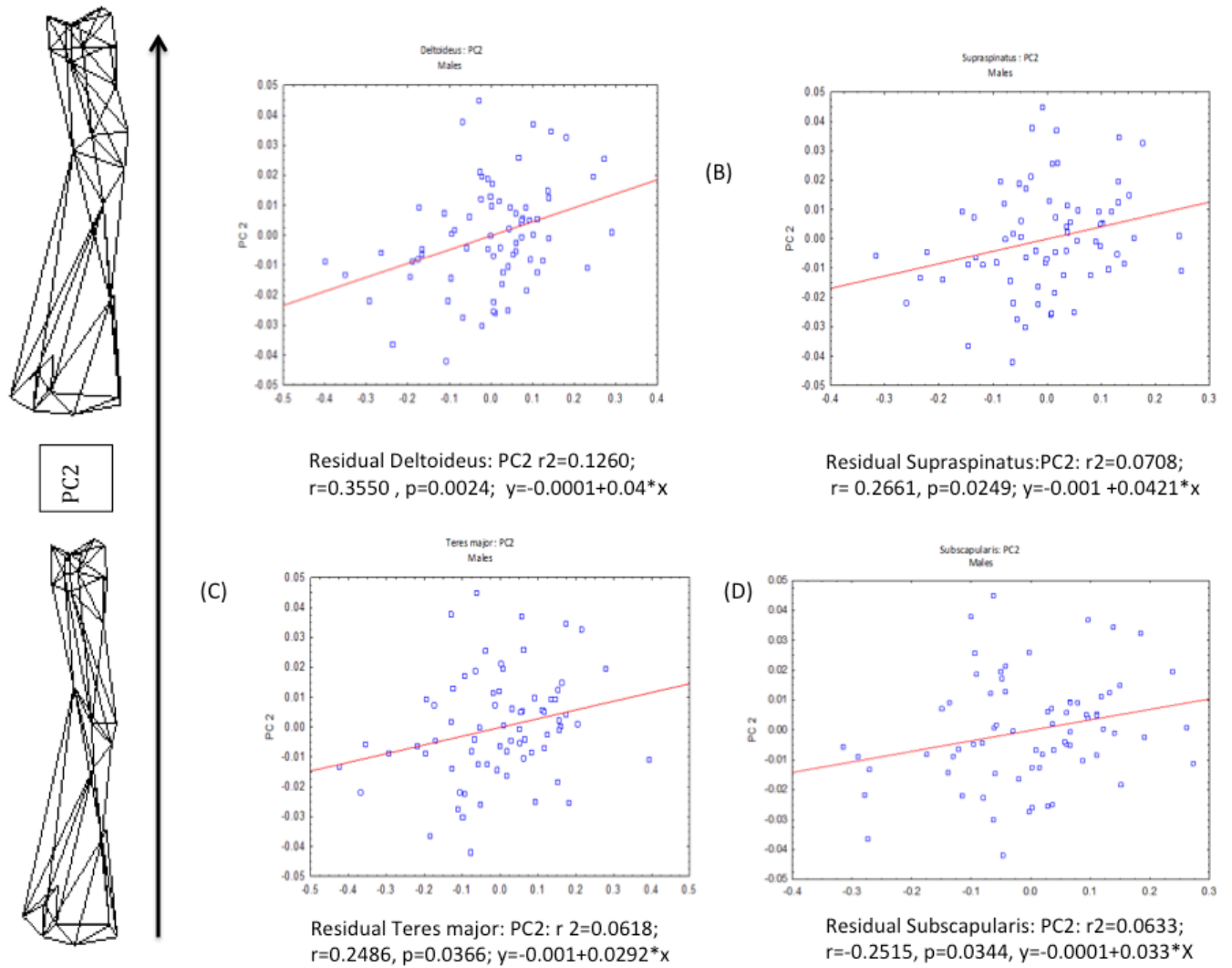


Figure 3.10. Two wireframes of a hypothetical humerus characterised by low PC (-0.05) and high PC (0.05) for PC2 and correlated muscles males only.

PC3 accounted for 7.3% of the total variation in the male-only dataset. The PC is characterised by changes in the tubercle height and breadth, lateral movement of pectoral crest and distal movement of the extension of the lateral epicondyle (Table 3.11). Males were evenly distributed over the PC and shape changes are dictated by wireframes (Figure 3.11). There were no muscles correlated with this PC (Table 3.8).

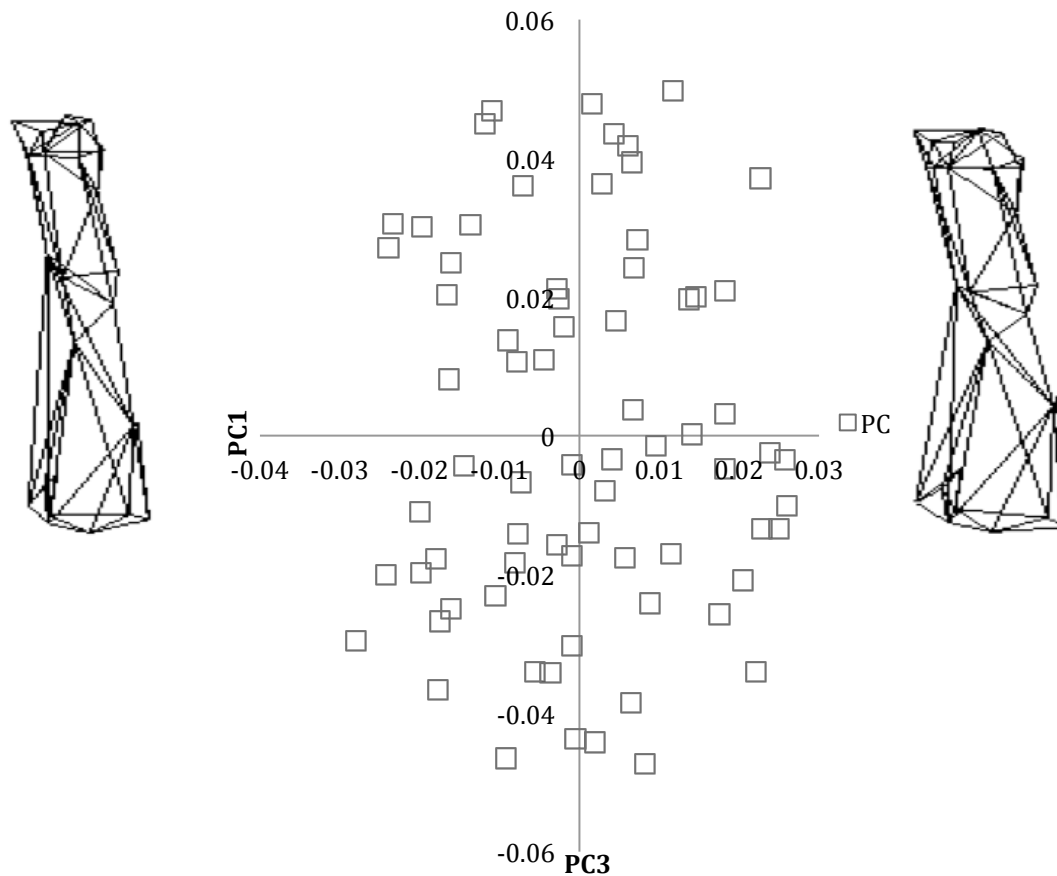


Figure 3.11. Two –dimensional scatter plot of PC3 on PC1, humeral Procrustes shape data. Males are represented by open squares. Wireframe shows expected shape at each extremity (left 0.03, right 0.03).

Table 3.11. Shape changes for PC3

Low PC score	High PC score
<ul style="list-style-type: none"> • Decreased tubercle size and breadth • Tubercles narrowed and became pointed • Inter-tubercle sulcus decreased in breadth • A less bulbous head at the level of the anatomical neck • Pectoral crest placed medially • Tuberosity on medial aspect placed proximally • Deltoid crest medially and distally placed • The extension of the lateral epicondyle on the distal epiphysis decreased in size and placed distally and medially 	<ul style="list-style-type: none"> • Increased tubercle size and breadth • Tubercles widened and flattened at proximal points • Inter-tubercle sulcus increased in breadth • Relatively bulbous head protruding away from the anatomical neck • Pectoral crest placed laterally • Tuberosity on medial aspect moved distally • Deltoid crest placed proximally and laterally • The extension of the lateral epicondyle on the distal epiphysis increased in size and placed proximally and laterally

PC4 accounted for 5.9% of the total variation in the male-only dataset. The PC is characterised by changes in roundness of the humeral head, narrowing of proximal points on tubercles, increased robustness of shaft movement of epicondyles resulting in a transversely narrower distal epiphysis (Table 3.12; Figure 3.13). Majority of males are located between the middle and higher PC scores though some are located at the lower PC scores, changes are visualised by wireframes (Figure 3.12). There were no muscles correlated with this PC (Table 3.8).

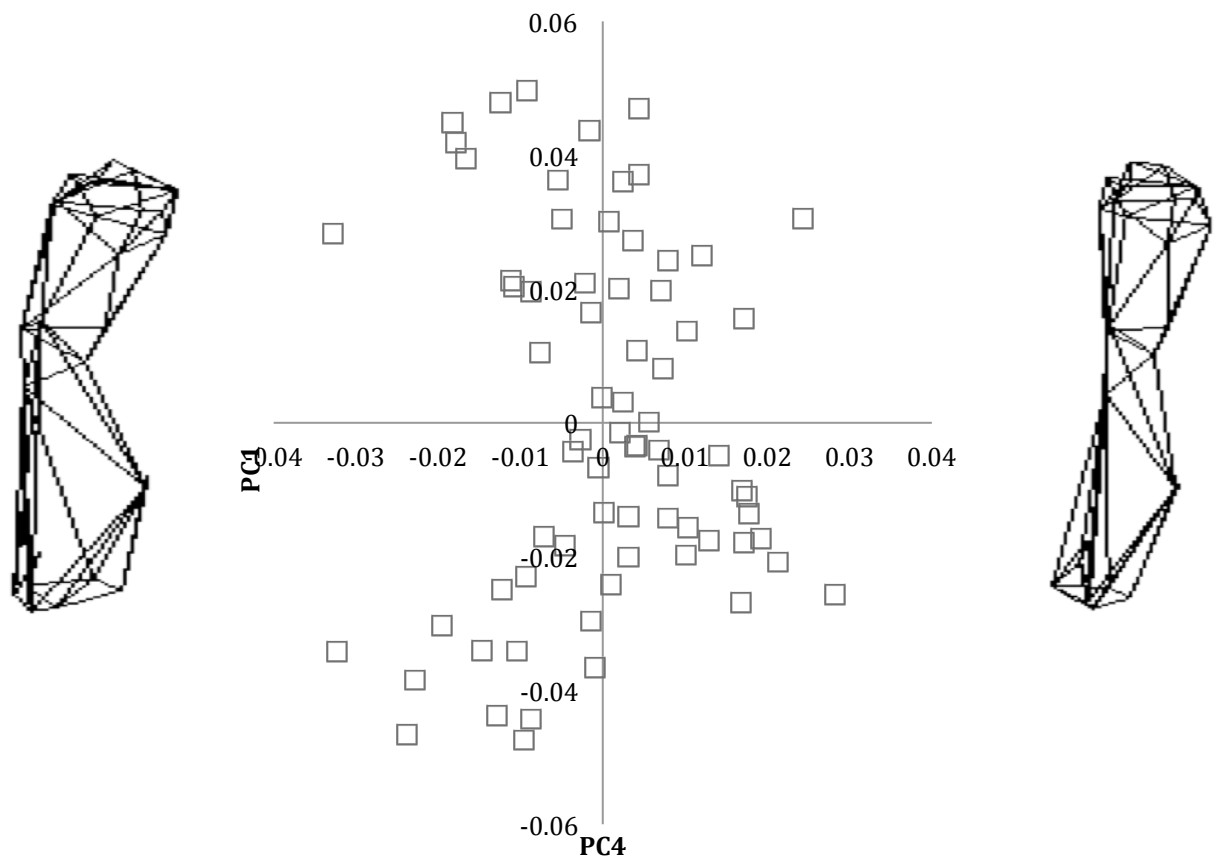


Figure 3.12. Two –dimensional scatter plot of PC4 on PC1, humeral Procrustes shape data., Males are represented by open squares. Wireframe shows expected shape at each extremity (left -0.04, right 0.03).

Table 3.12. Shape changes for PC4

Low PC score	High PC score
<ul style="list-style-type: none"> • Proximal placement of the roundness of the humeral head • Tubercles became broader and proximal points moved in a laterally • Inter-tubercle sulcus increased in breadth and length • Shaft became robust, torsion of the bone increased; relative lengthening of the top third • The pectoral crest was placed proximally • Deltoid crest placed dorsally • Medial tuberosity placed posteriorly • Lateral epicondyle placed proximally • Medial epicondyle placed distally • Extension of the lateral epicondyle increased in size and became lateral • The supracondyloid foramen was placed distally 	<ul style="list-style-type: none"> • Distal movement of the roundness of the humeral head • Tubercles became narrowed and proximal points placed in a medially • Inter-tubercle sulcus decreased in breadth and length • Shaft became less robust torsion of the bone decreased relative length of the top third shortened • The pectoral crest was placed distally the deltoid crest placed coronal • Medial tuberosity placed anteriorly • Lateral epicondyle placed distally • Medial epicondyle placed proximally • Extension of the lateral epicondyle decreased in size and placed medially • The supracondyloid foramen was placed proximally

PC5 accounted for 4.8% of the total variation in the male-only dataset. The PC is characterised by changes in the relative breadth of the proximal epiphysis, broadening of the shaft and lateral placement of deltoid crest along with increased relative breadth of the distal epiphysis (Table 3.13; Figure 3.13) There were significant correlations of residual muscle mass for this PC (Table 3.8; Figure 3.14).

Table 3.13. Shape changes for PC5

Low PC score	High PC score
<ul style="list-style-type: none"> • Decreased relative breadth, height and length at the proximal epiphysis • The medial tuberosity was placed distally • Shaft became narrower and deltoid crest was placed medially, and decreased in relative breadth • Extension of the lateral epicondyle increased and placed proximally 	<ul style="list-style-type: none"> • Increased relative breadth, height and length at the proximal epiphysis • The medial tuberosity on the shaft was placed proximally • Shaft is became broader • Deltoid crest was placed laterally • Distal epiphysis increased in relative breadth • Extension of the lateral epicondyle decreased and placed distally

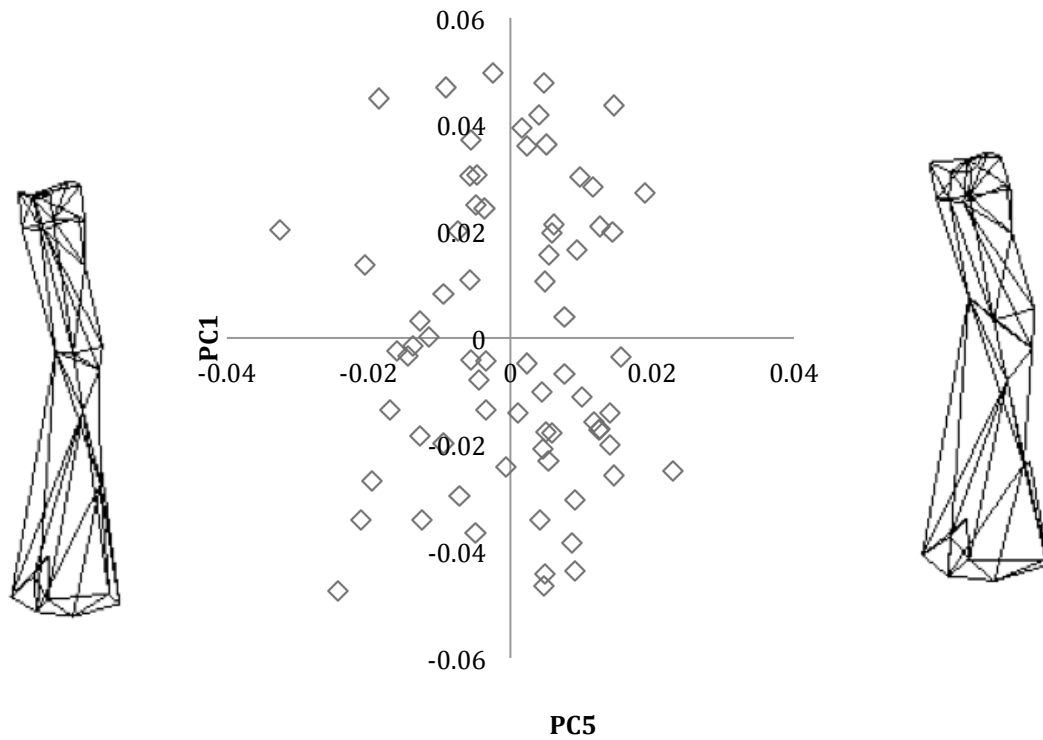


Figure 3.13. Two –dimensional scatter plot of PC5 on PC1, humeral Procrustes shape data., Males are represented by open squares. Wireframe shows expected shape at each extremity(left -0.04, right 0.03).

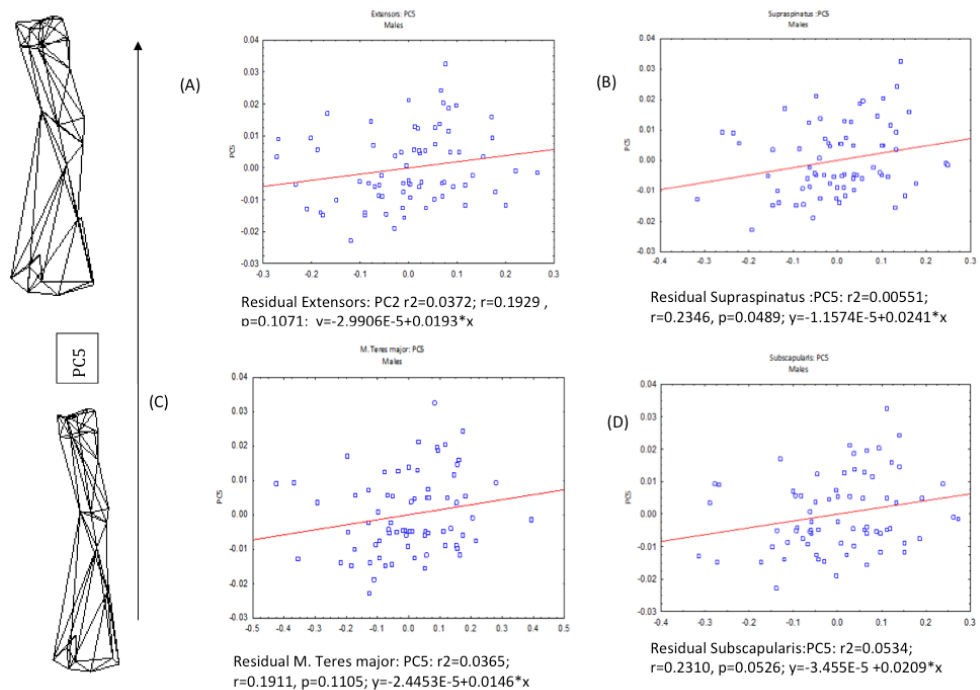


Figure 3.14. Two wireframes of a hypothetical humerus characterised by low PC (-0.04) and high PC (0.03) for PC5 and correlated muscles males only.

Females

There were eight PC factors scores that described the shape data for the female-only dataset. Of these, there were significant correlations with muscles for PC3, 4,5,6,7 and 8 (Table 3.14).

Table 3.14 Correlated Muscles and PC scores for females $p < 0.05$ ** $p < 0.01$ *** $p < 0.001$

PC	Correlated muscles
PC1 (22.2%)	N/A
PC2 (10.9%)	N/A
PC3 (10%)	<i>M. Biceps brachii</i> r^2 0.2423
PC4 (8.9%)	<i>M. Brachialis</i> r^2 0.3444 *
PC5 (6.7%)	<i>M. Brachialis</i> r^2 0.1105
PC6 (6.2%)	<i>M. Infraspinatus teres minor</i> r^2 0.3434 *
PC7 (5.6%)	<i>M. Deltoideus</i> r^2 0.3483 * <i>M. Infraspinatus teres minor</i> r^2 0.3304 * <i>M. brachialis</i> r^2 0.1057 <i>M. Tricep brachii</i> r^2 0.1356
PC8 (4.4%)	<i>M. Supraspinatus</i> r^2 0.3454 * <i>M. Triceps brachii</i> r^2 0.2745 * <i>M. Infraspinatus teres minor</i> r^2 0.4383 **

PC1 accounted for 22.2% of the variation in the female-only data set. The PC is characterised by the changes in tubercle proximity, distal placement of deltoid crest, elongation of the top third of the shaft and distal placement of the extension of the lateral epicondyle (Table 3.15; Figure 3.15). There were no significant muscles correlated with this PC.

Table 3.15. Shape changes for PC1

Low PC score	High PC score
<ul style="list-style-type: none">• Medial placement of proximal points of the tubercles• Proximal placement of deltoid and pectoral crest• Shortening of the top third of the shaft• Proximal placement of the extension of the lateral epicondyle and increased relative size• The supracondyloid foramen is placed proximally	<ul style="list-style-type: none">• Tubercles moved closer in proximity• Proximal and lateral placement of proximal points• Distal placement of the deltoid and pectoral crests• Elongation of the top third of the shaft is observed• Extension of the lateral epicondyle relatively decreased in size and is placed distally• The supracondyloid foramen is placed distally

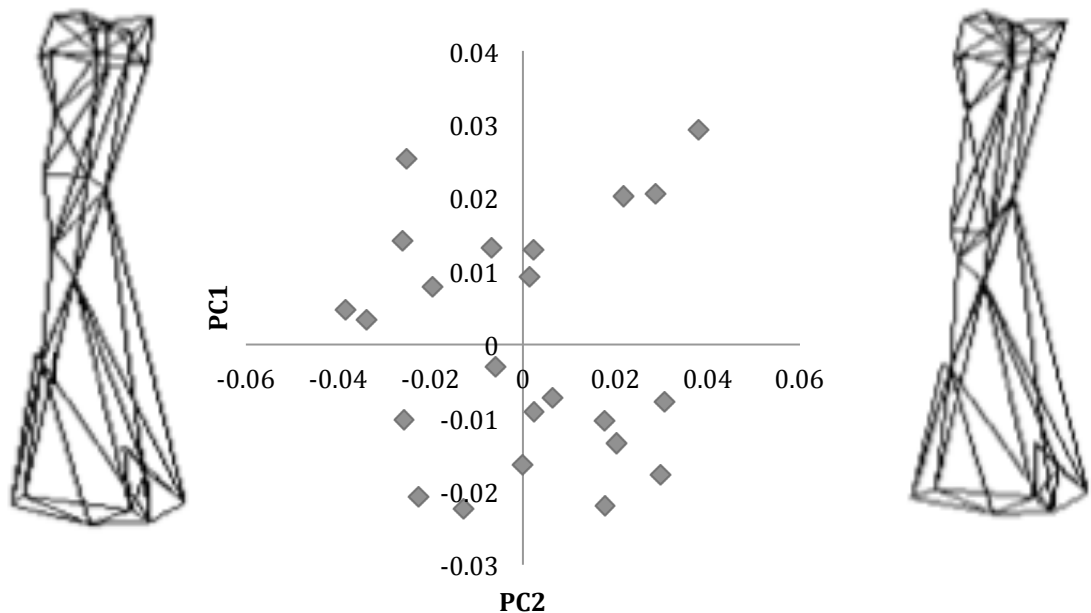


Figure 3.15. Two –dimensional scatter plot of PC2 on PC1, humeral Procrustes shape data. Females represented by shaded diamonds. Wireframe shows expected shape at each extremity (left -0.04, right 0.04).

PC2 accounted for 10.9% of the variation in the female-only data set. The PC is characterised by the changes in the width of the humeral head, elongation of the greater and lesser tubercle, relatively narrow shaft and (Table 3.16; Figure 3.16).

The PC2 was correlated with centroid size ($p < 0.0001$) (Figure 17). There were no muscles correlated with this PC (Table 3.14).

Table 3.16. Shape changes for PC2

Low PC score	High PC score
<ul style="list-style-type: none"> • Relatively wide humeral head • Tubercles became relatively shortened • Tuberosity on the medial side of the shaft is moved laterally • Relatively more robust shaft, flexion is observed • Relative decrease in width of the capitulum and trochlea also placed distally • The inferior aspect of the trochlea is placed distally resulting in a backwards flexion of the distal epiphysis 	<ul style="list-style-type: none"> • Relatively narrow humeral head • Tubercles became relatively elongated, medial placement of the medial tubercle • Relatively narrow shaft • Flexion is observed due to the bending • The capitulum and the trochlea increased laterally and proximally • The inferior aspect of the trochlea is placed proximally resulting in an upward flexion

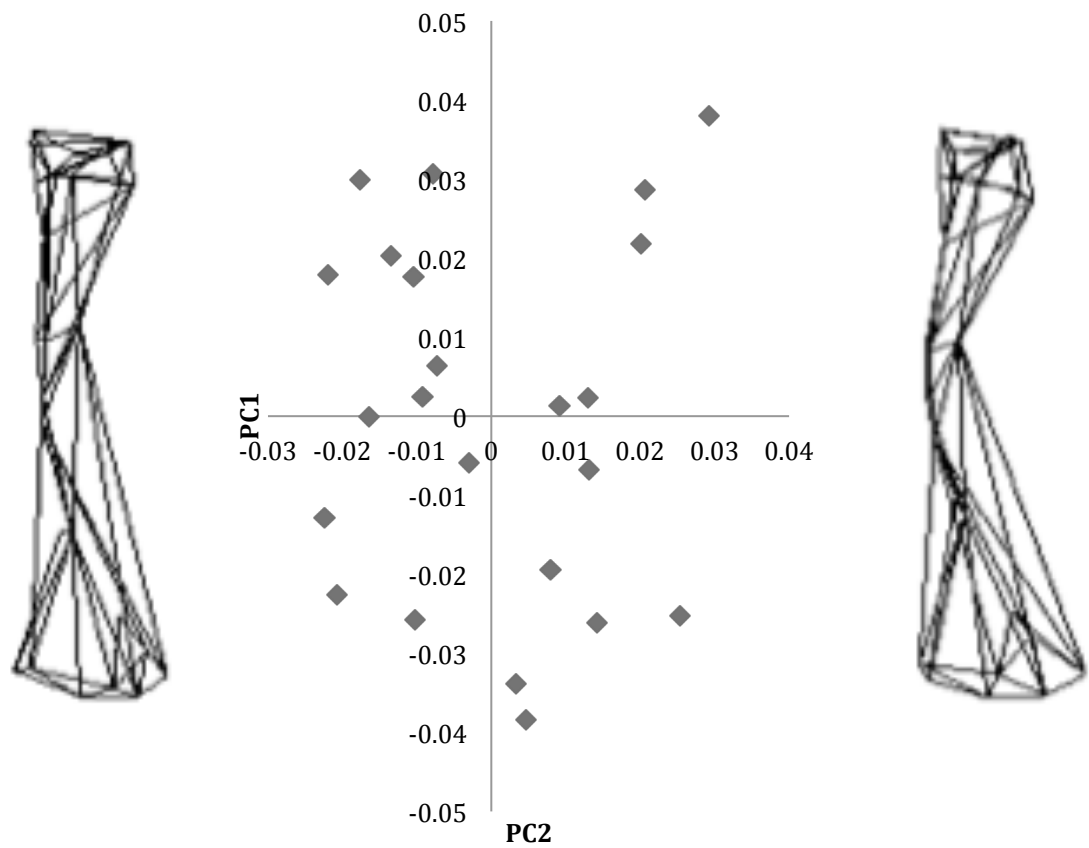


Figure 3.16. Two –dimensional scatter plot of PC1 on PC2, humeral Procrustes shape data. Females represented by shaded diamonds. Wireframe shows expected shape at each extremity (left -0.03, right 0.04).

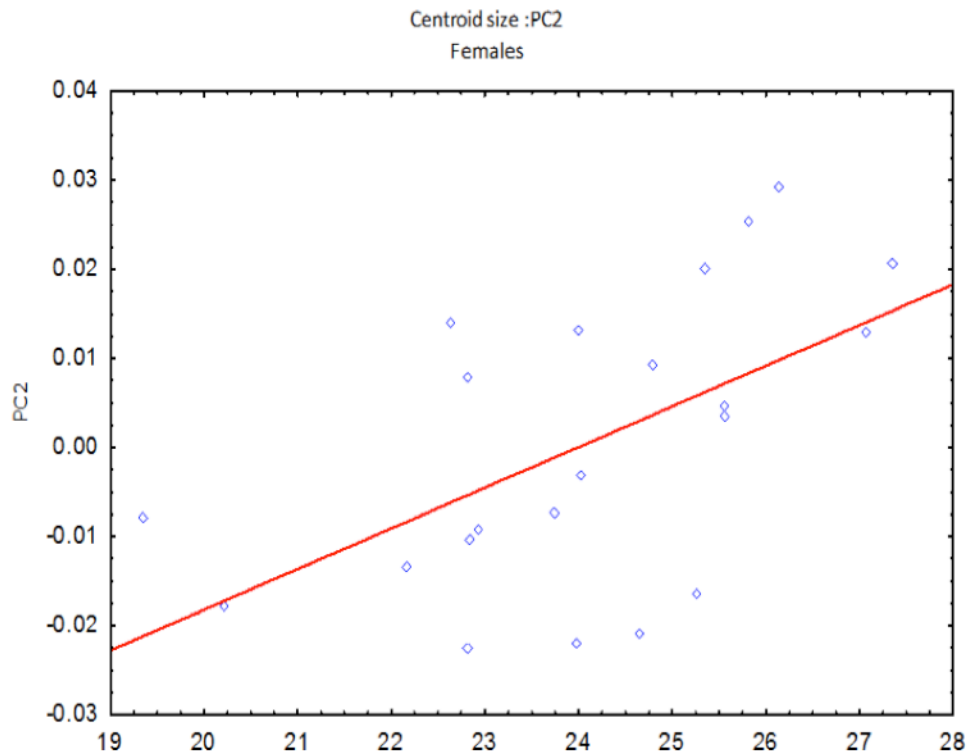


Figure 3.17: Centroid size correlated to PC2 for females.

PC3 accounted for 10% of the variation in the female-only data set. The PC is characterised by the changes in relatively broader humeral head with increased breadth and height of inter-tubercle sulcus, laterally placed pectoral crest and proximally placed deltoid crest. Distal epiphysis has movement of the lateral epicondyle and inferior aspect of the trochlea broadened laterally (Table 3.17; Figure 3.18). Females were distributed between high and low PC scores. There were significant correlations of residual muscle mass for this PC (Table 3.14; Figure 3.19).

Table 3.17. Shape changes for PC3

Low PC score	High PC score
<ul style="list-style-type: none"> • Narrower tubercles and the proximal points are placed proximally • Inter-tubercle sulcus decreased in breadth and height • The tuberosity of the medial aspect is placed laterally • The pectoral crest is placed medially and distally in the anterior aspect, the deltoid crest is placed distally • The supracondyloid foramen of the distal epiphysis is placed proximally • The lateral epicondyle moved medially and distally • The inferior aspect of the trochlea narrowed medially 	<ul style="list-style-type: none"> • Relatively broader tubercles and laterally placement of proximal points • Increased breadth and height of inter-tubercle sulcus • The tuberosity of the medial aspect was medially placed • The pectoral crest is placed laterally and proximally in the anterior aspect • The deltoid crest is placed proximally and the arch of the crest is became smaller bending of the shaft also occurred. The supracondyloid foramen of the distal epiphysis is placed distally • The lateral epicondyle is placed laterally and proximally • The inferior aspect of the trochlea broadened laterally

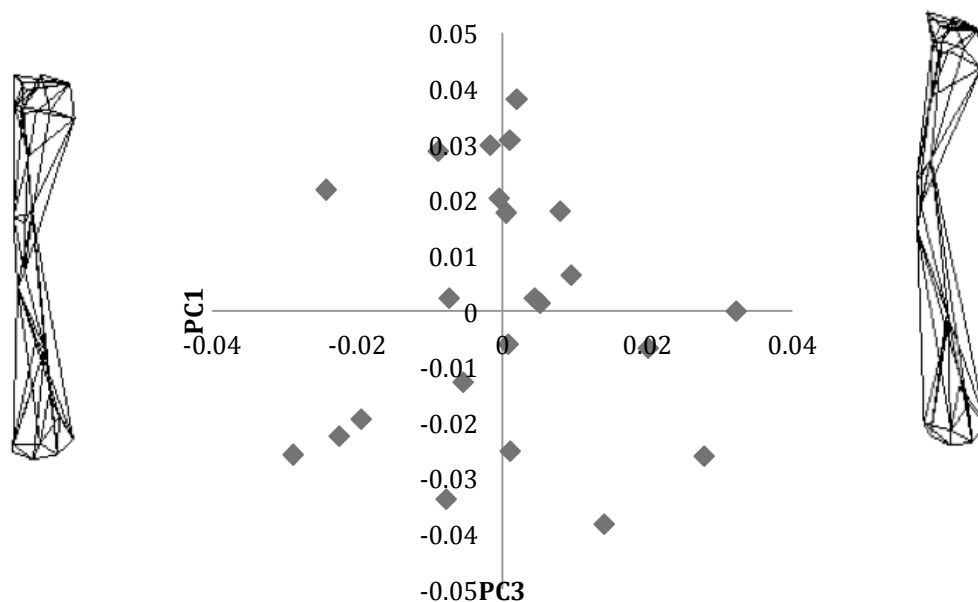


Figure 3.18. Two –dimensional scatter plot of PC3 on PC1, humeral Procrustes shape data. Females represented by shaded diamonds. Wireframe shows expected shape at each extremity (left -0.04, right 0.04).

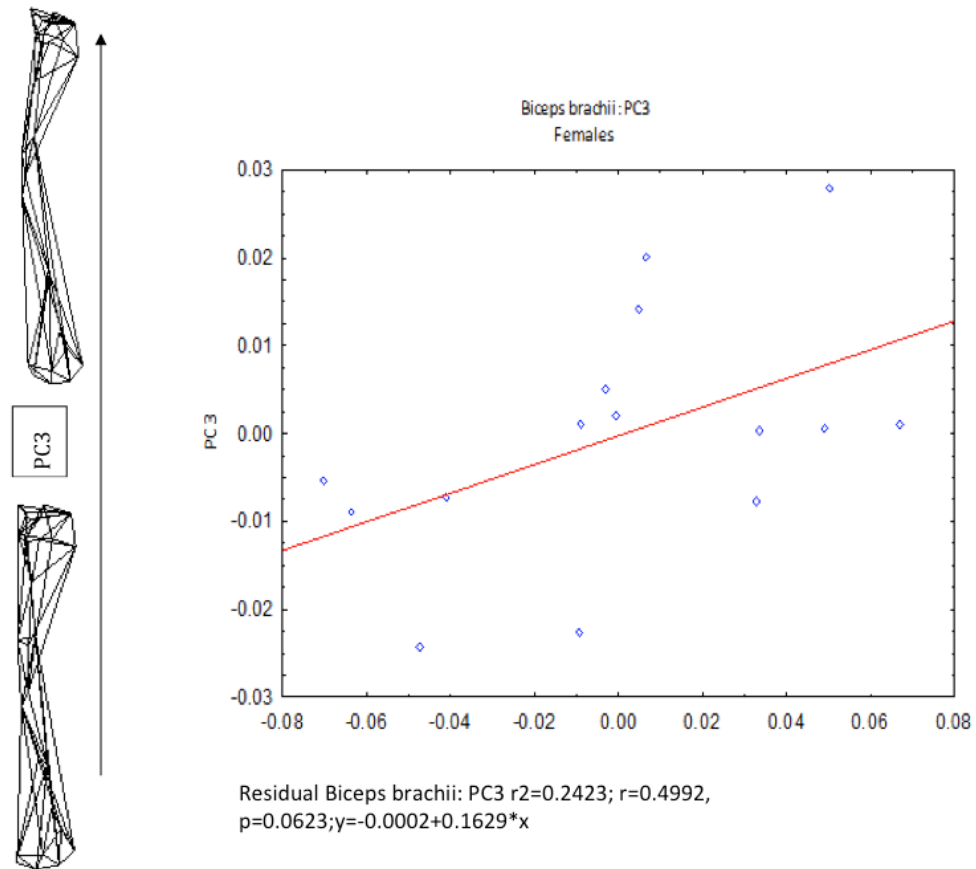


Figure 3.19. Two wireframes of a hypothetical humerus characterised by low PC (-0.04) and high PC (0.04) for PC3 and correlated muscles females only.

PC4 accounted for 10.9% of the variation in the female-only data set. The PC is characterised by the changes in relative height and breadth of the humeral head and the elongation of the shaft (Table 3.18; Figure 3.20). Females were distributed towards high PC scores with only a few individuals lying in the low PC score area. There were significant correlations of residual muscle mass for this PC (Table 3.14; Figure 3.21).

Table 3.18. Shape changes for PC4

Low PC score	High PC score
<ul style="list-style-type: none"> • Relatively shorter and broader humeral heads • Torsion of the bottom third of the humeral shaft and increased thickness and shortening of the shaft • Lateral epicondyle is placed anteriorly 	<ul style="list-style-type: none"> • Relative increased height and breadth of humeral head • The shaft became longer, thinner and straighter

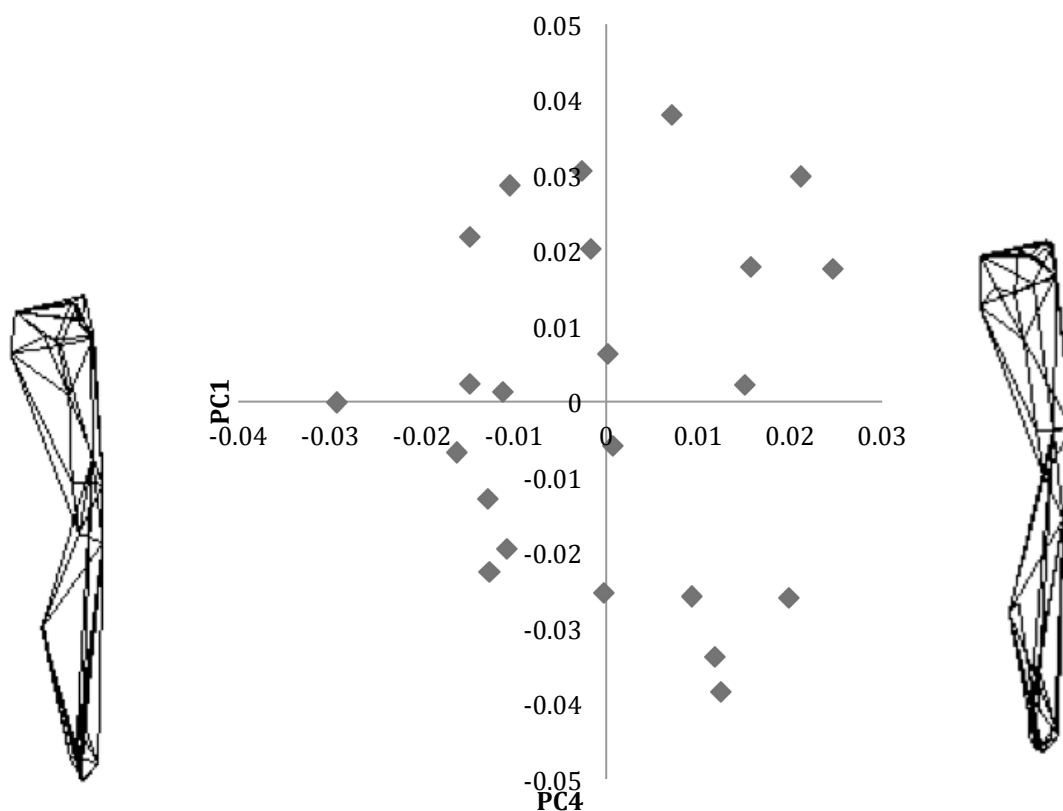


Figure 3.20. Two –dimensional scatter plot of PC4 on PC1, humeral Procrustes shape data. Females represented by shaded diamonds. Wireframe shows expected shape at each extremity (left -0.04, right 0.03).

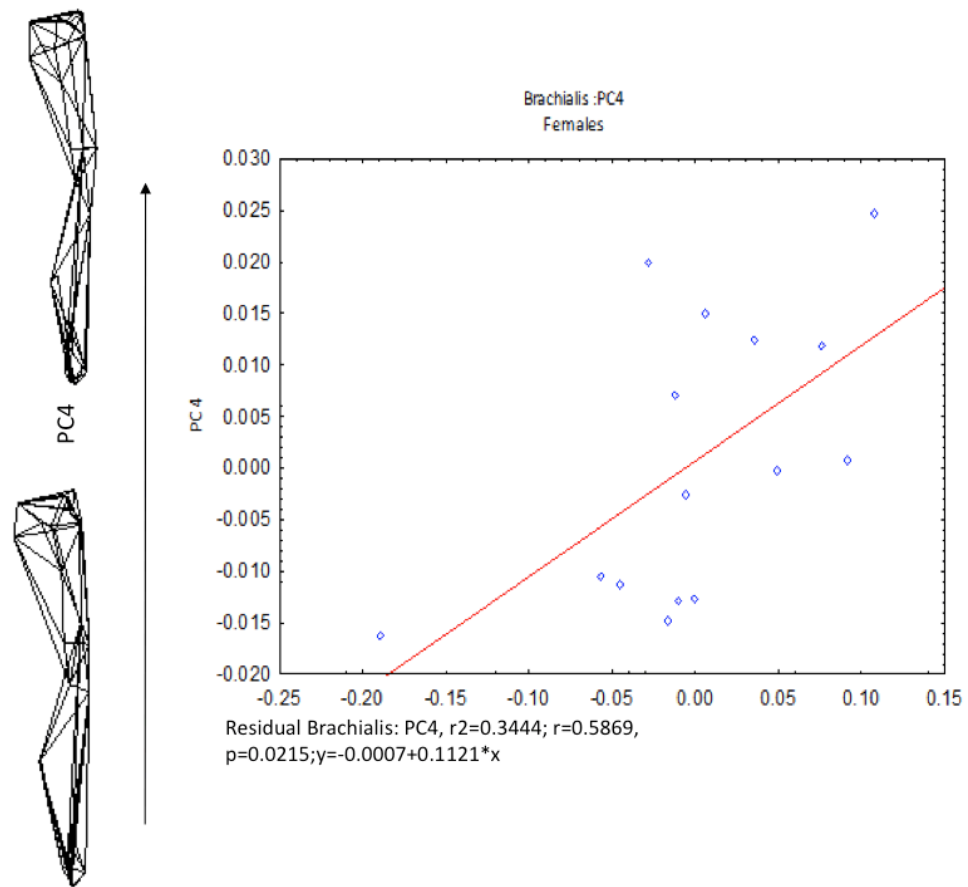


Figure 3.21. Two wireframes of a hypothetical humerus characterised by low PC (-0.03) and high PC (0.03) for PC4 and correlated muscles females only.

PC5 accounted for 6.7% of the variation in the female-only data set. The PC is characterised by the changes in a relatively more bulbous humeral head, medial placement of tubercles, distal placement of deltoid crest, flattening of inlet between medial epicondyle and trochlea and proximal and lateral placement of the lateral epicondyle (Table 3.19; Figure 3.22). There were significant correlations of residual muscle mass for this PC (Table 3.14; Figure 3.23).

Table 3.19. Shape changes for PC5

Low PC scores	High PC scores
<ul style="list-style-type: none">• A less bulbous head at the level of the anatomical neck• Tubercles are placed laterally and most proximal points flattened• The superior aspect of the trochlea and capitulum are placed medially• The supracondyloid foramen is placed proximally• The inlet between the medial epicondyle and the trochlea is concave• The lateral epicondyle is placed distally and medially	<ul style="list-style-type: none">• Relatively bulbous head protruding away from the anatomical neck• Tubercles also placed medially and most proximal points placed proximally• The deltoid crest is flexing posteriorly• Distal placement of the deltoid crest.• Lateral placement of the superior aspect of the trochlea and capitulum, distal placement of the supracondyloid foramen• The inlet between the medial epicondyle and the trochlea flattened• Proximal and lateral placement of the lateral epicondyle• The trochlea also broadens on the inferior aspect

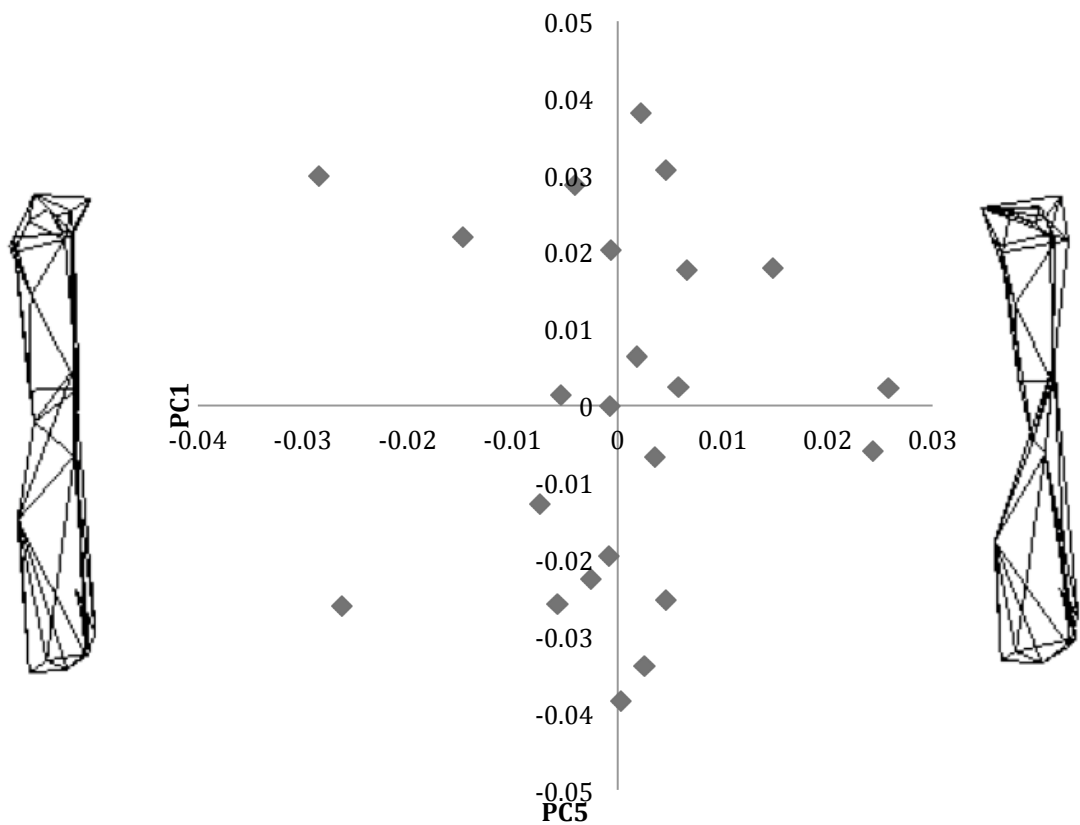


Figure 3.22. Two –dimensional scatter plot of PC4 on PC1, humeral Procrustes shape data. Females represented by shaded diamonds. Wireframe shows expected shape at each extremity (left -0.03, right 0.03)

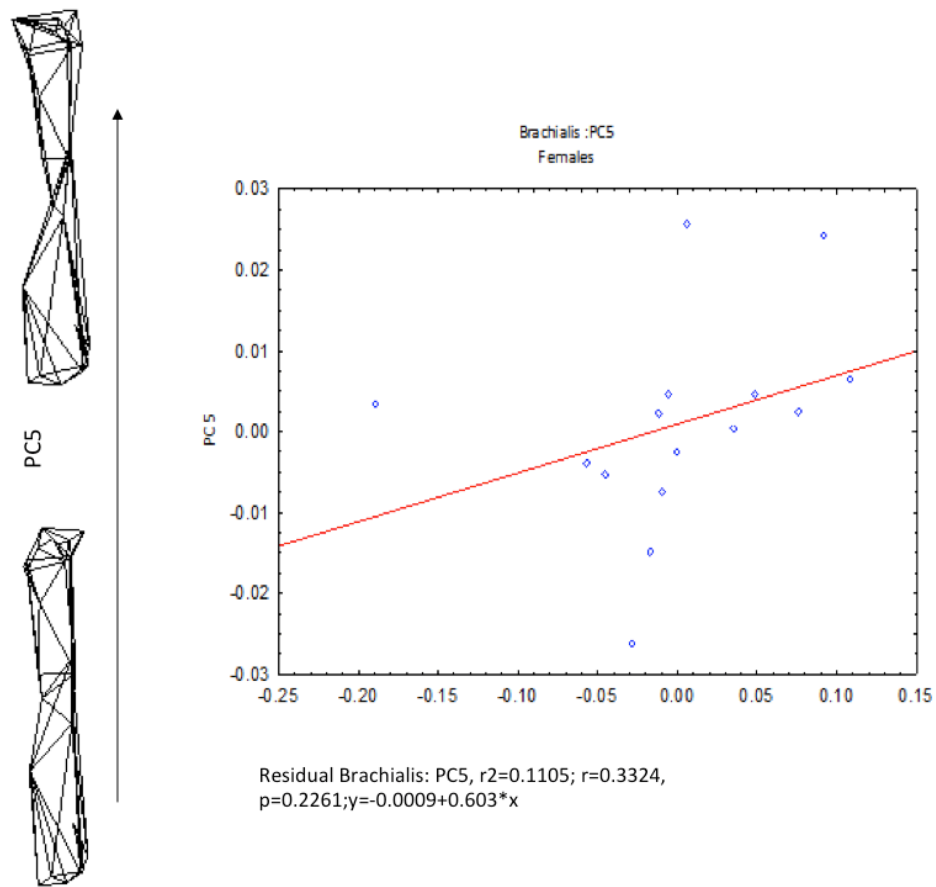


Figure 3.23. Two wireframes of a hypothetical humerus characterised by low PC (-0.03) and high PC (0.03) for PC5 and correlated muscles females only.

PC6 accounted for 6.2% of the variation in the female-only data set. The PC is characterised by changes in the breadth of the humeral head, lateral movement of the greater and lesser tubercles, distal placement of the deltoid crest, and relatively broad distal epiphysis (Table 3.20; Figure 3.24). There were significant correlations of residual muscle mass for this PC (Table 3.14; Figure 3.25).

Table 3.20. Shape changes for PC6

Low PC score	High PC score
<ul style="list-style-type: none"> • Head and breadth relatively decreased in size • The tubercles are placed medially • Inter-tubercle sulcus increased in size, head is also become less bulbous • The deltoid crest is placed proximally and the over all shaft became relatively gracile. • The distal epiphysis became relatively narrow • The extension of the lateral epicondyle and medial condyle are placed medially 	<ul style="list-style-type: none"> • Relative increased head size and breadth • The tubercles moved laterally, inter-tubercle sulcus decreased in size head is also become more bulbous • The deltoid crest is placed distally and the over all shaft became relatively robust • The distal epiphysis relatively broadens • The extension of the lateral epicondyle is placed laterally • The medial epicondyle also placed laterally

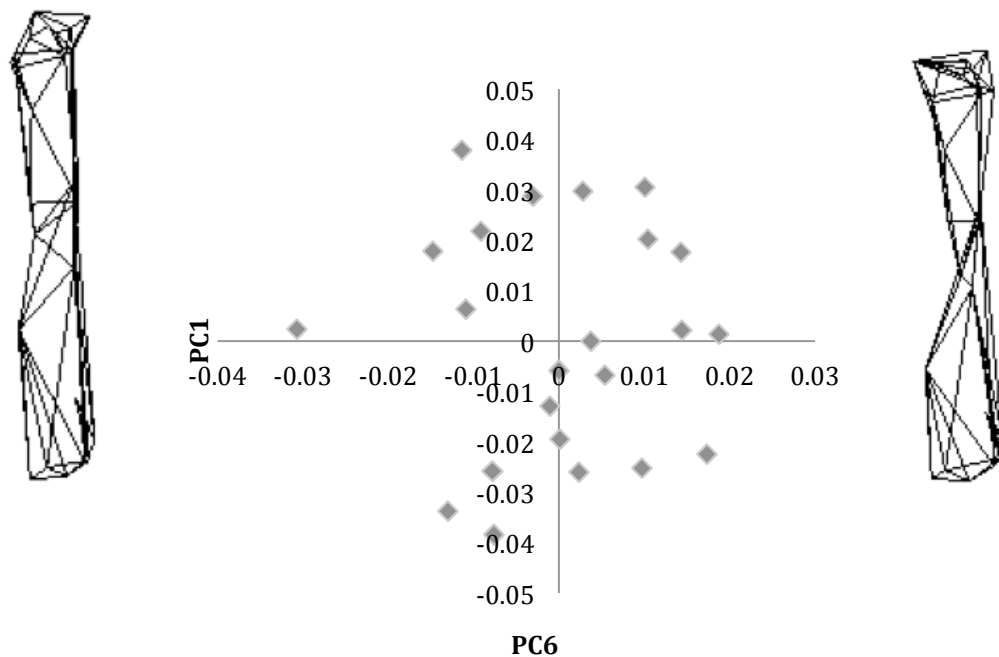


Figure 3.24. Two –dimensional scatter plot of PC6 on PC1, humeral Procrustes shape data. Females represented by shaded diamonds. Wireframe shows expected shape at each extremity (left -0.03, right 0.02).

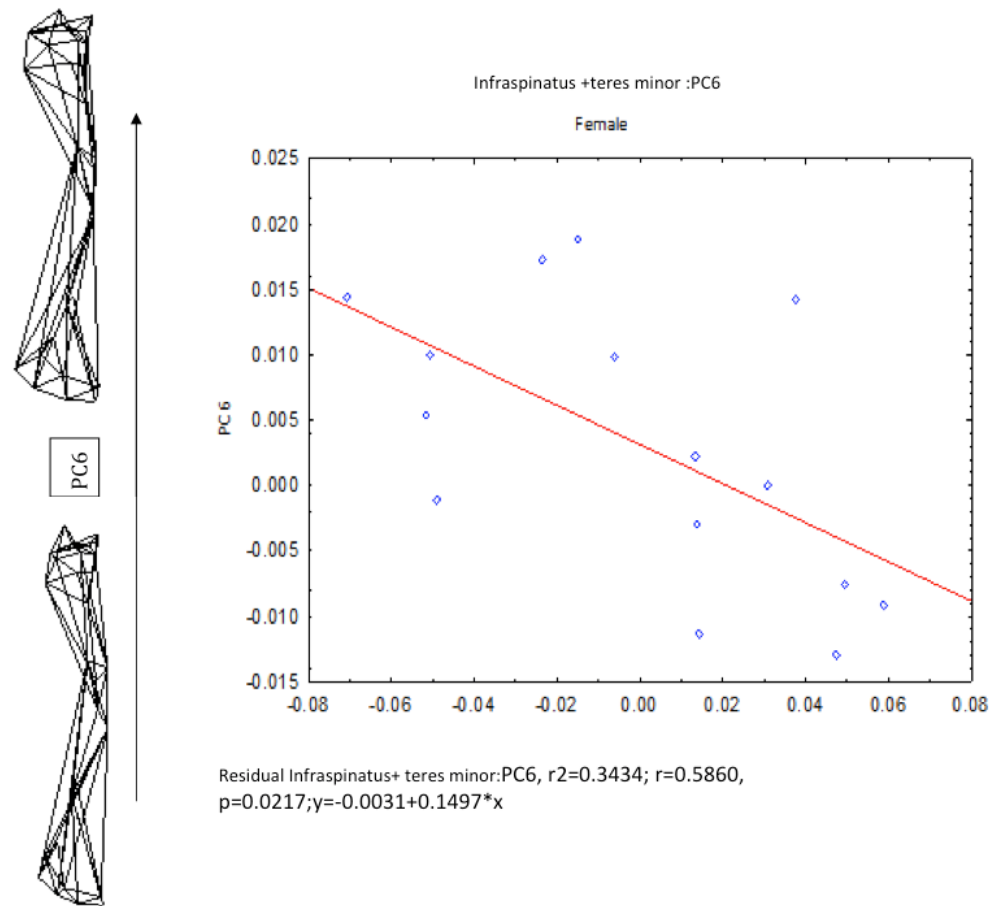


Figure 3.25. Two wireframes of a hypothetical humerus characterised by low PC (-0.03) and high PC (0.02) for PC6 and correlated muscles females only.

PC7 accounted for 5.6% of the variation in the female-only data set. The PC is characterised by changes in the greater and lesser tubercle, lateral placement of the pectoral crest, medial placement of the lateral epicondyle and lateral placement of the medial epicondyle (Table 3.21; Figure 3.26). There were significant correlations of residual muscle masses for this PC (Table 3.14; Figure 3.27).

Table 3.21. Shape changes for PC7

Low PC scores

- Greater and lesser tubercles became narrower and proximal points are placed medially
- The pectoral crest is placed medially in the anterior plane narrowing the shaft
- The lateral epicondyle is placed laterally and the medial epicondyle is placed medially and distally
- The inferior aspect of the trochlea became narrower and decreased medially

High PC scores

- Greater and lesser tubercles became broadened and proximal points placed laterally, the greater tubercle are however placed more extremely
- The pectoral crest is placed laterally in the anterior plane thickening the shaft
- The lateral epicondyle is placed medially and the medial epicondyle is placed laterally and proximally
- The inferior aspect of the trochlea broadened and increased laterally

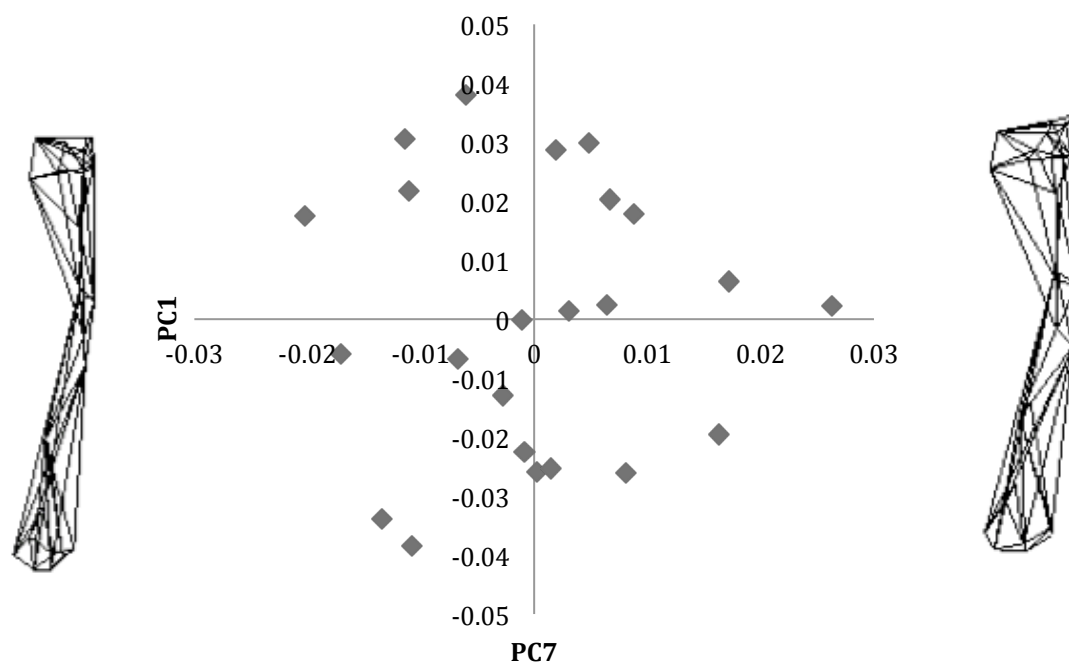


Figure 3.26 Two -dimensional scatter plot of PC7 on PC1, humeral Procrustes shape data. Females represented by shaded diamonds. Wireframe shows expected shape at each extremity (left -0.03, right 0.03).

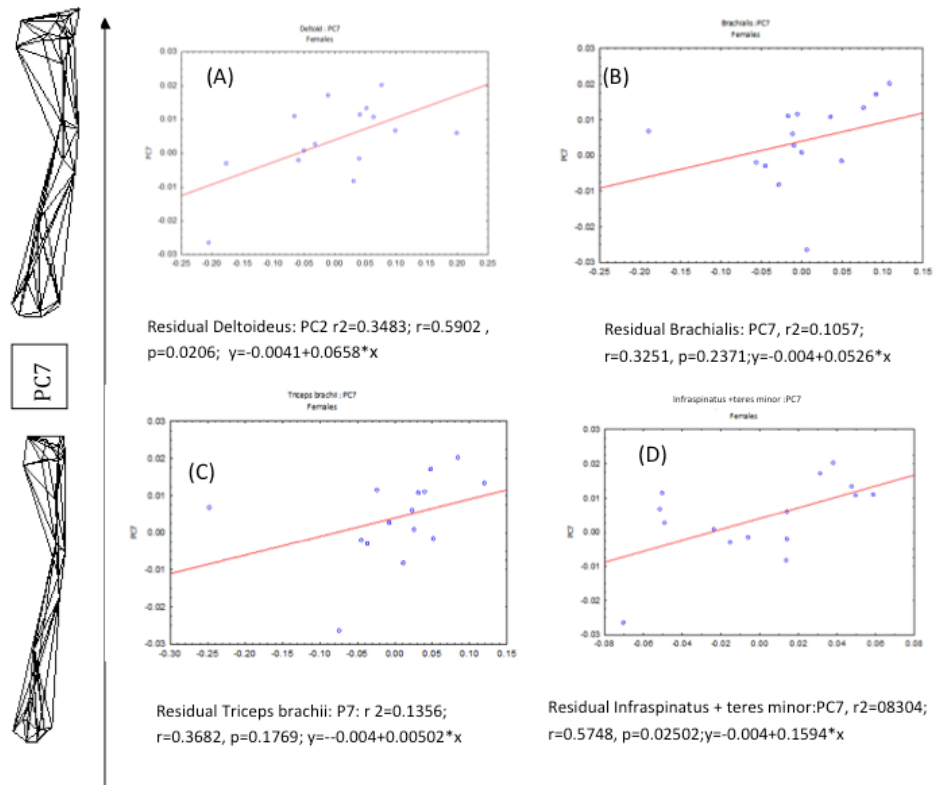


Figure 3.27 Two wireframes of a hypothetical humerus characterised by low PC (-0.03) and high PC (0.03) for PC7 and correlated muscles females only.

PC8 accounted for 4.4% of the variation in the female-only data set. The PC is characterised by the changes in relatively smaller greater tuberosity, enlarged lesser tubercle, medial and proximal placement of the medial tuberosity and transversely widened distal epiphysis (Table 3.22; Figure 3.28). There were significant correlations of residual muscle masses for this PC (Table 3.14; Figure 3.29).

Table 3.22. Shape changes for PC8

Low PC scores

- Relatively larger greater tuberosity and laterally placed
- The most posterior point became relatively pointed
- The lesser tubercle decreased in size and posterior points are placed distally
- The inter tubercle sulcus became anterior and relatively increased in size
- The medial epicondyle is laterally and distally placed
- Transversely widened distal epiphysis

High PC scores

- Relatively smaller greater tuberosity and became medially placed
- The most posterior point became relatively flat
- The lesser tubercle enlarged and posterior points are placed proximally
- The inter tubercle sulcus became posterior and relatively decreased in size
- The medial epicondyle is medially and proximally placed
- Transversely widened distal epiphysis

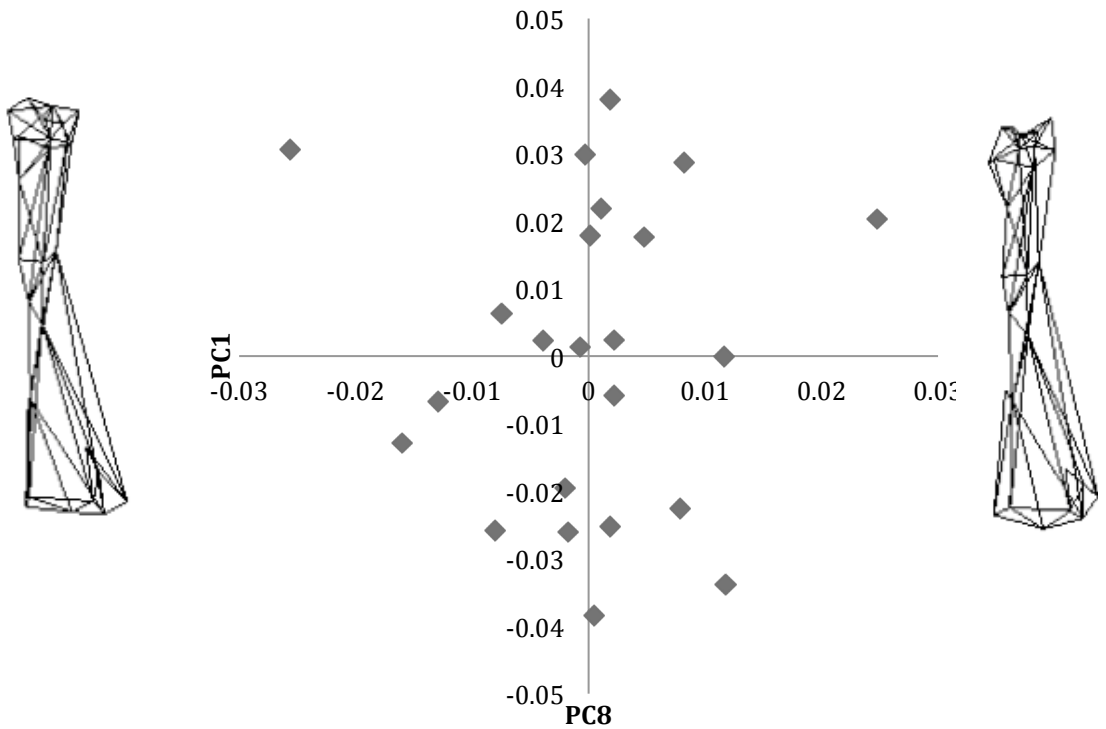


Figure 3.28 Two –dimensional scatter plot of PC8 on PC1, humeral Procrustes shape data. Females represented by shaded diamonds. Wireframe shows expected shape at each extremity (left -0.03, right 0.03).

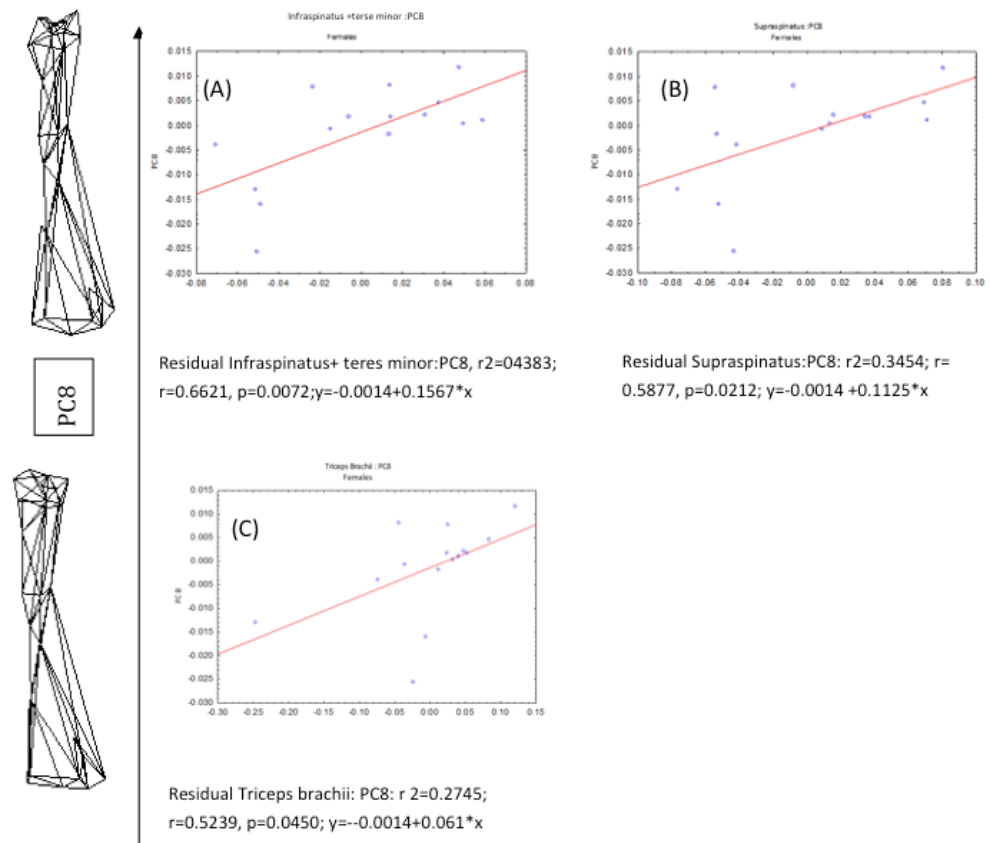


Figure 3.29. Two wireframes of a hypothetical humerus characterised by low PC (-0.03) and high PC (0.03) for PC8 and correlated muscles females only.

Chapter Four : Discussion

4.1 Humeral shape in kangaroos: allometric effects

Highly significant size and shape dimorphism was apparent in the sample examined. As body size increases (especially for males), muscle mass increases and influences the shape of the humerus. For the combined data set (males and females) centroid size was correlated with PC1, indicating that as the humerus increased in size, the morphology of the bone changes accordingly. As the humerus increases in size the relative size of the greater tuberosity, deltoid and pectoral crest become increasingly enlarged; this may be due to the positive allometry displayed by the forelimb muscles. The distal end of the humerus displays isometric growth (PC1 scores becomes positive the epiphysis becomes relatively wider), although the positions of the medial and lateral epicondyle change: the lateral epicondyle is placed more distally in larger bones and the medial epicondyle increases in width. These overall changes in humerus shape are likely to reflect changing forces acting on the bones due to the increased musculature in larger males.

Interestingly, when males and females were analysed separately, the allometric patterns were not the same. For the male data set, centroid size was correlated to PC1, which captured changes in the humeral head, shaft and distal epiphysis. These changes are the same observed for the combined-sex data set, except for the medial epicondyle that is seen to medially expand, this may be due to the greater male sample size, therefore creating a male bias in the data. For the female data set, centroid size was correlated with PC2. This PC factor captured changes in the

humeral head, shaft and distal epiphysis, which were all observed to narrow, except the lateral increase of the trochlea and capitulum and along with the flexion of the distal epiphysis. The correlation with centroid size indicated that size plays a role in the determination of shape in males and females. Males and females exhibit different allometric patterns of growth, which contribute to differences in musculature and therefore contribute to the difference in shape within males and females.

When comparing the male- and female-only datasets, there are similarities in the bending of the humeral shaft though the extent of this bending is very different. There are however, more differences, especially in the humeral head. The tubercles of male-only dataset are observed to decrease in width and height and also flatten where female tubercles are observed to elongated and have a more narrowed points. The bulbous characteristic between females and males are also different with the male becoming less bulbous as the PC increases and females becoming more bulbous as the PC increases. This is interesting, as joint surfaces are correlated to forces associated with weight bearing during pentapedal movement but the muscle attachments are increasing in size at a lower rate.

For the humerus shaft, the pectoral and deltoid crests become more laterally extended as size increases and the shaft of appears to become flexed and 'twisted'. These changes are more exaggerated in males than females. As the magnitude of stress increases, the distance from the axis of rotation, and the maximum stress caused by sheer forces acts both perpendicularly and parallel to the axis of the bone (Ruff *et al.* 2006, Frost 2009). This bending is correlated with muscle mass,

as the force and loading increases the bone modifications to accommodate this stimulus.

The morphological changes between males and females are different at specific sites of the humerus, which is likely to reflect the difference in muscle growth between males and females. The positive allometry in males has seen a difference in size of the tubercles and deltoid and pectoral crest in relation to the increase in size of the humerus, whereas females exhibit an isometric change in the proportion of the bone as the bone increases. The distal epiphysis for the male and female data set is similar as the PC becomes higher the distal epiphysis increases in relative width; therefore, as size increases the distal epiphysis becomes wider. However the extension of the lateral epicondyle is different between males and females. The movement of the extension is the same in each sex, although the height of the extension differs. In males, the extension is distally placed, whereas in females, the extensions are proximally placed. The morphology of the bone is therefore seen to change in response to increases in size. There are also differences in the movements of the trochlea and capitulum; moving closer in proximity in males and further in females. In females, the flexion of the distal epiphysis is also present (absent in males).

4.2 Bone shape related to muscularity

The residual muscles that are correlated with the bone changes in the male-only dataset are *m. deltoideus*, *m. supraspinatus*, *m. subscapularis*, *m. teres major* and the extensor groups. The origins and insertions of these muscles are mainly around

the pectoral and deltoid crest, where the humerus shape changes occur. Muscle-generated forces have an impact on bone shape as modelling changes occur due to stimuli (Nigg *et al.* 2007). For the bone to remain architecturally stable, the bone has to even out the compression and tensile forces acting on the bone (Nigg *et al.* 2007, Currey 2014). The changes observed for males on either side of the shaft (*m. deltoideus* and *m. teres major*) could suggest that the bone is responding to the increased muscularity of the muscles, therefore modelling to reflect the stimuli (Nigg *et al.* 2007, Currey 2014). Similarly, the extensor groups play a role in the shape change of the distal epiphysis. This muscle group are associated with the lateral epicondyle; therefore the extensors may influence the increased breadth of the distal epiphysis but may also influence the position of the lateral epicondyle as it is observed to extend distally in males. Extensor muscles are associated with the extension of the forearm; the rapid movement of the male forearm in ritual sparing increases the muscularity of these muscles and therefore the increased mass this creates additional force on the bone and therefore influencing the position of the lateral epicondyle.

For females, humerus shape changes were correlated with the residual masses of the *m. biceps brachii*, *m. brachialis*, *m. infraspinatus* + *m. teres minor*, *m. supraspinatus*, *m. deltoideus* and *triceps brachii*. The shape changes that occurred were associated with the humeral head, distal shaft and distal epiphysis. *M. supraspinatus*, *m. infraspinatus* and *m. teres minor* muscle groups, may influence the greater tubercle, due to its increased size. The deltoideus muscle is associated with the change occurring at the deltoid crest, the deltoid crest widened as the PC

increased. *M. brachialis* is likely to affect the width of the distal epiphysis. This infers that females with higher muscularity have increased distal epiphyseal width.

The muscularity of males and females were observed to affect shape changes in the humeri. As muscularity increased for both sexes, the shape change increased.

These shape changes are more pronounced in males than females and this may also be a part of the positive allometric growth of males in comparison to isometric growth in females.

4.3 Can we predict sex of individual from humeral shape?

The sexual dimorphic nature of the humerus can be used in order to distinguish between male and female kangaroos. The accuracy associated with this is very high (92%). The parts of the humerus that expressed the greatest degree of sexual dimorphism were the relative size and shape of the proximal tubercles, deltoid crest, and the distal epiphysis. Greater developments of the tubercles are an indication of a relatively more muscular individual especially in the shoulder muscles resulting from the positively allometric growth of forelimb muscles in male kangaroos (Warburton *et al.* 2013). Though due to the sex biased present in our sample this needs to be considered when we look at sex estimation, as the sample is predominately male.

Males and females can be distinguished by their tubercles by the most proximal points: male tubercles are flattened while females are pointed. Differences in the shape of the proximal point may be an indication of the *m. supraspinatus*, *m.*

infraspinatus and *m. subscapularis* muscles attaching to the humerus and the amount of loading they put onto the tubercle. This difference in loading may be due to the allometric and isometric growth between males and females. The deltoid crest can also be used to distinguish the differences between males and females due to the exaggerated presence in males. As the size of the bone increased the relative size of the deltoid crest increased. As males attain a larger size (normally 1.5 times heavier than females), a more pronounced deltoid crest, which is laterally placed is indicative of a male. Vance *et al.* (2012) indicated there was vast variation in the robusticity of the distal humerus in the South African population, meaning there is lots of variation within the humerus of the South African population, the medial epicondyle showed great variance between males and females, which led to greater degree of sex estimation (Vance *et al.* 2013). Although Vance *et al.* (2013) indicated there was vast differences in the robustness of the distal humerus between males and females, in our investigation the size of the distal epiphysis increased for both sexes, this may be due to kangaroos also being bipeds and pentapeds, as they have relatively smaller anterior scapula area, shorter humeri and more proximally placed deltoid tuberosity and wider epicondyle (Price 1993). The presence of wider epicondyles was supported by this investigation and agreed with Price's (1993) findings where the medial and lateral epicondyle for males and females were placed laterally. Differences however occurred for the extension of the lateral epicondyle. Males exhibited a more distal and lateral placed extension and was relatively decreased in length, where female lateral epicondyles are proximally and laterally placed and increase in relative length. This is another way to distinguish males from females. Males and females can therefore be differentiated by the characteristics the bone displays

4.4 Limitations and future research

Aspects of this study that could have been improved was sample size. The small number of female humeri used in this investigation was less than half the size of the male sample, therefore as seen a male bias in the sample and the female sample may have been under-represented. Another way we could have improved our study was by the use of computer tomography (CT). This method allows for very precise allocation of landmarks and thus results in a more accurate investigation. The methods we have used can be applied to various other biological samples such as quenda and bandicoot. Investigating the sexual dimorphic nature of the kangaroo humerus may allow possible insight to the understanding of sexual selection of the humerus and the role it plays in kangaroo populations. The current investigation can also be further extended to incorporate other members of the *Macropus* genus such as *M. rufus* and *M. giganteus*. By incorporating these groups into this study, it has the potential to determine whether similar shape differences occur between species.

Chapter 5: Conclusions

The ability for bone to functionally change to external stimuli like muscles is vital to meet the ever-changing demands of the skeleton (Sommerfeldt *et al.* 2001).

When prompted to stimuli, bones can change, remodel due to functional loading to suit life events, such as increased muscle development (Currey 2014). In context of Wolff's Law, the effects of residual muscle masses influence humerus shape in the western grey kangaroo, with male muscles showing more observable effects than females due to the relative differences in muscle growth.

No study has completed geometric morphometrics on the kangaroo humerus or included fine dissection muscle data. Some studies, however, have studied the relationship between the effects of muscles on bone shape (e.g. Cornette *et al.* 2015). This study has demonstrated that sexual dimorphism is exhibited in the *Macropus fuliginous* humerus by geometric morphometrics and the effect muscles have in their relationship with bone shape.

Investigating the sexually dimorphic nature of the kangaroo humerus allows the understanding of sexual selection and the role it plays in kangaroo populations. Due to males monopolising females, male kangaroos highly invest heavily in muscle development compared to females. This investment has seen an impact on bone shape in relation to different sexes. My hypothesis is supported that there is sexual dimorphic difference in the shape of western grey kangaroo humeri and the positive ability to predict sex from bone is highly discriminatory. The effects of muscles differ in males and females; this difference thus has influence on the bone

shapes displayed between males and females. The different growth rates have placed different forces onto the bone, which have caused a morphological change. The sexual behaviour of males may also influenced the shape of the bone as it has a positive relationship with muscle mass,. Males are categorised by having a more robust humeral shaft and bending due to increased muscle forces acting on the bone. Conversely females attain a more gracile humerus and grow isometrically. As muscles grow at the same rate in females, the stimuli of stress on the bone is potentially even and therefore the bone responds in a equivalent manner thus the bone changes observed are less noticeable than in the males. Females also do not participate in ritual sparing fights and therefore the need for increased muscularity is less necessary thus contributing to a more gracile humerus. As indicated in our study, sexual dimorphism is present in western grey kangaroo humeri and is influenced by muscle mass.

References

- Abouheif, E. and Fairbairn, D. J. (1997). "A comparative analysis of allometry for sexual size dimorphism: assessing Rensch's rule." American Naturalist: 540-562.
- Adams, D. C., *et al.* (2004). "Geometric morphometrics: ten years of progress following the 'revolution' " Italian Journal of Zoology **71**:1: 5-16.
- Andersson, M., and Iwasa, Y. (1996). "Sexual selection." Trends in Ecology & Evolution **11**(2): 53-58.
- Argot, C. (2001). "Functional - adaptive anatomy of the forelimb in the didelphidae, and the paleobiology of the paleocene marsupials Mayulestes ferox and Pucadelphys andinus." Journal of Morphology **247**(1): 51-79.
- Birkhead, T. R., and Møller, A. P. (1998). "Sperm competition and sexual selection". Academic Press.
- Bisazza, A., *et al.* (2001). "Female mate choice in a mating system dominated by male sexual coercion." Behavioral Ecology **12**(1): 59-64.
- Bonduriansky, R. (2007). "Sexual selection and allometry: a critical reappraisal of the evidence and ideas." Evolution **61**(4): 838-849.
- Bookstein, F. L. (1997). Morphometric tools for landmark data: geometry and biology, Cambridge University Press.
- Clutton-Brock, T. and McAuliffe , K. (2009). "Female mate choice in mammals." The Quarterly Review of Biology **84**(1): 3-27.
- Clutton-Brock, T. H. and Parker, G. A. (1995). "Sexual coercion in animal societies." Animal Behaviour **49**(5): 1345-1365.
- Cooke, S. B. and Terhune, C. E. (2015). "Form, function, and geometric morphometrics " The Anatomical record **298**: 5-28.
- Cornette, R., *et al.* (2015). "The shrew tamed by Wolff's law: Do functional constraints shape the skull through muscle and bone covariation?" Journal of Morphology **276**(3): 301-309.
- Cowin, S. C. (2001). "Bone mechanics handbook." CRC press LLC
- Croft, D. B., and Snaith, F. (1991). "Boxing in red kangaroos, macropus rufus: aggression or play?" international journal of Comparative Psychology **4**: 221-236.
- Currey, J. D. (2014). The mechanical adaptations of bones, Princeton University Press.
- De Lisle, S. P., and Rowe,L. (2013). "Corelated evolution of allometry and sexual dimorphism across higher taxa." The American naturalist **182**(5): 630-639.
- Dryden, I. L. and Mardia, K. V. (1998). Statistical shape analysis, Wiley Chichester.
- Franklin, D., *et al.* (2007). "Sexual dimorphism in the subadult mandible: quantification using geometric morphometrics " Journal of Forensic Science **52**(1): 6-10.

- Frost, H. M. (2009). "Wolff's Law and bone's structural adaptations to mechanical usage: an overview for clinicians." The Angle Orthodontist **64**(3) : 175-188
- Galef, B. G., *et al.* (2008). "Evidence of mate choice copying in norway rats, *Rattus norvegicus*." Animal Behaviour **75**(3): 1117-1123.
- Goodship, A., and Cunningham, J. (2001). "Pathophysiology of functional adaptation of bone in remodelling and repair in-vivo." In: Bone Mechanics Handbook (2nd Ed.). Boca Raton, London, New York, Washington DC: CRC Press, 26.1-26.31
- Grigg, G. C., *et al.* (1989). Kangaroos, wallabies and rat-kangaroos, Chipping Norton , NSW: Surrey Beatty & Sons Pty limited.
- Hood, C. S., (2000). "Geometric morphometric approaches to the study of sexual size dimorphism in mammals." Hystrix **11**(1): 77-90.
- Hopwood, P., and Butterfield, R., (1990). "The Locomotor Apparatus of the Crus and Pes of the Eastern Gray Kangaroo, *Macropus-Giganteus*." Australian Journal of Zoology **38**(4): 397-413.
- Hopwood, P. R. (1974). "The intrinsic musculature of the pectoral limb of the Eastern Grey Kangaroo (*Macropus major* (Shaw) *Macropus giganteus* (Zimm))." Journal of Anatomy **118**(Pt 3): 445.
- Hosken, D. J., and House, C. M. (2011). "Sexual selection." Current Biology **21**(2): R62-R65.
- Isaac, J. L.(2005)."Potential causes and life-history consequences of sexual size dimorphism in mammals." Mammal review **35**(1): 101-115.
- Jarman, P. (1983). "Mating system and sexual dimorphism in large terrestrial mammalian herbivores." Biological Reviews **58**(4): 485-520.
- Jarman, P. (1989). b. Sexual dimorphism in Macropodoidea. . Chipping Norton, NSW: , Surrey Beatty & Sons Pty Ltd
- Johnson, C. (1983). "Variations in Group Size and Composition in Red and Western Grey Kangaroos, *Macropus rufus* (Desmarest) and *M. fuliginosus* (Desmarest)." Wildlife Research **10**(1): 25-31.
- Lammers, A. R. *et al.* (2001). "Ontogeny of sexual dimorphism in *Chinchilla lanigera* (Rodentia: Chinchillidae)." Journal of Mammalogy **82**(1): 179-189.
- Lane, M. (2014). Sperm competition and sexual selection in Western Grey kangaroos *Macropus fuliginosus*. School of Veterinary and life Sciences. Murodoch University, Murodoch University.
- Marcus, L. F., *et al.* (2013). Advances in morphometrics, Springer Science & Business Media.
- Marieb, E. and K. Hoehn (2010). Human anatomy and physiology.(8th), San.

- McCracken, K. G., *et al.* (2000). "Sexual size dimorphism of the Musk Duck." The Wilson Bulletin **112**(4): 457-466.
- McPherson, F. J., and Chenoweth, P. J. (2012). "Mammalian sexual dimorphism." Animal Reproduction Science **131**: 109-122.
- Miller, E. J., *et al.* (2010). "Dominance, body size and internal relatedness influence male reproductive success in eastern grey kangaroos (*Macropus giganteus*)." Reproduction, Fertility and Development **22**(3): 539-549.
- Miller, W. C., *et al.* (1990). "Diet composition, energy intake, and exercise in relation to body fat in men and women." The American journal of clinical nutrition **52**(3): 426-430.
- Nigg, B. M., and Herzog, W. (2007). Biomechanics of the musculo-skeletal system, John Wiley & Sons Ltd, The atrium Southern Gate, Chichester: West Sussex.
- O'Higgins, P. (2000). "The study of morphological variation in the hominid fossil record: biology, landmarks and geometry." Journal of Anatomy **197**: 103-120.
- O'Higgins, P., and Jones, N. (1999). "Morphologika." Tools for shape analysis. University College London, London, United Kingdom.
- Pearson, O. M. and Lieberman, D. E. (2004). "The aging of Wolff's "law": ontogeny and responses to mechanical loading in cortical bone." American journal of physical anthropology **125**(S39): 63-99.
- Price, M. V. (1993). "A functional - morphometric analysis of forelimbs in bipedal and quadrupedal heteromyid rodents." biological journal of the Linnean Society **50**(4): 339-360.
- Rensch, B. (1959). Evolution above the species level, Columbian Univ. Press. New York.
- Richards, H., *et al.* (2015). "Strong arm tactics: sexual dimorphism in macropodid limb proportions." Journal of Zoology.
- Rieucou, G., *et al.* (2012). "investigating differences in vigilance tactic use within and between the sexes in eastern grey kangaroos." PloS ONE **7**(9).
- Rip (2008). "Rip's Applied Mathematics Blog: PCA / FA example 2: jolliffe. discussion 3: how many PCs to keep?" Rip's Applied Mathematics Blog. Retrieved 1st october 2015.
- Rodger, J., and White, I. (1975). "Electroejaculation of Australian marsupials and analyses of the sugars in the seminal plasma from three macropod species." Journal of reproduction and fertility **43**(2): 233-239.
- Rubenstein, D. I., and Wrangham, R. W. (1986). Ecological aspects of social evolution, Princeton UP Princeton (NJ).
- Rubin, C. T. (1984). "Skeletal strain and the functional significance of bone architecture." Calcified tissue international **36**(1): S11-S18.
- Ruff, C., *et al.* (2006). "Who's afraid of the big bad Wolff?: "Wolff's law" and bone functional adaptation." American journal of physical anthropology **129**(4): 484-498.

- Sargis, E. J. (2002). "Functional morphology of the forelimb of tupaiids (Mammalia, Scandentia) and its phylogenetic implications." Journal of Morphology **253**(1): 10-42.
- Scott, E. M., *et al.* (2005). "Aggression in bottlenose dolphins: evidence for sexual coercion, male-male competition, and female tolerance through analysis of tooth-rake marks and behaviour." Behaviour **142**(1): 21-44.
- Simmons, L. W. (2005). "The evolution of polyandry: sperm competition, sperm selection, and offspring viability." Annual Review of Ecology, Evolution, and Systematics: 125-146.
- Slice, D. E., (2007). "geometric morphometrics." Annual Reviews **36**: 261-281.
- Slice, D. E., *et al.* (2009, 12th February 2009). "a glossary for geometric morphometrics." Retrieved 23rd february 2015, from <http://life.bio.sunysb.edu/morph/glossary/gloss1.html>.
- Soltistis, J., *et al.* (1997). "Sexual selection in Japanese macaques I: female mate choice or male sexual coercion?" Animal Behaviour **54**(3): 725-736.
- Sommerfeldt, D. and Rubin, C. (2001). "Biology of bone and how it orchestrates the form and function of the skeleton." European Spine Journal **10**(2): S86-S95.
- Soulsbury, C. D., *et al.* (2014). "Sexual size dimorphsim and the strength of sexual selection in mammals and birds." Evolutionary ecology research **16**: 63-76.
- Stockley, P., *et al.* (1997). "Sperm competition in fishes: the evolution of testis size and ejaculate characteristics." The American naturalist **149**(5): 933-954.
- Trivers, R. (1972). Parental investment and sexual selection. Pages 136–179 in B. Campbell, ed. *Sexual selection and the descent of man, 1871–1971*, Aldine, Chicago.
- Vance, V. and Steyn, M. (2013). "Geometric morphometric assessment of sexually dimorphic characteristics of the distal humerus." HOMO-Journal of Comparative Human Biology **64**(5): 329-340.
- Von Cramon-Taubadel, N., *et al.* (2007). "The problem of assessing landmark error in geometric morphometrics: theory, methods, and modifications." American journal of physical anthropology **134**(1): 24.
- Warburton, N. M., *et al.* (2013). "Sexual selection on forelimb muscles of Western Grey kangaroos (skippy was clearly female)." biological journal of the Linnean Society **109**: 923-931.
- Warburton, N. M., *et al.* (2011). "Functional morphology of the forelimb of living and extinct tree - kangaroos (*Marsupialia: Macropodidae*)." Journal of Morphology **272**(10): 1230-1244.
- Zelditch, M. L., *et al.* (2012). Geometric morphometrics for biologists: a primer, Academic Press.

7 Appendices

Appendix 1.

Definitions: Geometric Morphometrics.

All definitions have been collated from (Slice, Bookstein et al. 2009)

Term	Definition	Purpose
Allometry	Any change in shape with size.	The equation $y/x=c$ shows any deviation of the bivariate relation.
Canonical variates analysis C.V.A.	Method of multivariate analysis which the variation among groups of expressed relative to the pooled within group covariance matrix	Finds linear transformations of the data which maximises the among group variation relative to the pooled within group variation
Centroid size	Is the square root of the sum of squared distances of a set of landmarks from their centroid	Is used in G.M. because is uncorrelated with every shape variable. It is also used to scale configurations so they can be plotted as points in Kendall's shape space.
Cluster analysis		Expressed as a dendrogram, represents multivariate variation in a data as a series of sets.
Coordinates	A set of parameters that locate a point in geometrical space	
Discriminate analysis D.A.	A broad class of methods concerned with the development of rules for assigning unclassified objects to previously defined groups	Allows to assign unclassified object to previously defined groups
Euclidean distance matrix analysis. E.D.M.A.	A method for the statistical analysis of full matrices of all inter-landmark distances, averaging element wise within sample and then comparing those averages between samples by computing ratios of corresponding mean distances.	Coordinate free approach for comparing biological samples
Euclidean space	A space where distances between two points are defined as Euclidean distances in some system coordinates	
Finite element scaling analysis F.E.S.A.		Solves inverse problem for estimating the strains representing the hypothetical forces that deformed one specimen to another

Form	Form of an object by a point in space of form variables	Allows measurement of geometric objects
Generalised superimposition	Superimposition of a set of configurations onto their consensus configuration	Allows to affine transformations
Generalised Procrustes Analysis G.P.A	See Procrustes method	-
Geometric Morphometrics G.M.	Analysis of multivariate statistical data from Cartesian coordinates which are denoted from specific landmarks on a specimen	-
Homology	Discrete geometric structures, such as points or curves, and, by a further extension, to the multivariate descriptors that arise as part of the multivariate analysis	
Kendall's shape space	Fundamental geometric construction by David Kendall.	Provided a complete geometric setting for analyses of Procrustes distances among arbitrary sets of landmarks
Landmark	A specific point on a biological form or image of a form located according to some rule	Allows us to specifically identify a specific point in space.
Least squares estimate L.S.E	Parameter estimated that minimises the sum of squared differences between observed and predicted values.	-
Likelihood ratio test	Test based on the ratio of likelihood	Likelihood a specific hypothesis is true
Multivariate analysis of variance M.A.N.O.V.A	Analysis of variance of two or more dependent variables considered simultaneously	
Multivariate regression	The prediction of two or more dependent variable using one independent variable	
Multivariate multiple regression	The prediction of two or more dependent variable using two or more independent variable	
Partial least squares P.L.S	Is a multivariate statistical method for assessing relationships among two or more sets of variables measured on the same entities.	Is sued to analyses the covariance between the sets of variables.

Principal components analysis P.C.A	Set of vectors that are orthogonal both with respect to the identity matrix and the sample covariance matrix.
----------------------------------------	---------------------------------------------------------------------------------------------------------------

Procrustes distance	Approximately the square root of the sum of squared differences between the position of the landmarks in two optimally superimposed configuration at centroid size	Defines the metric for Kendall's space.
Procrustes method	A term for least squares methods for estimating nuisance parameters of the Euclidean similarity transformations.	Is usually the known as the method of least differences as a means for comparing homologous points on various specimens
Shape	The geometric properties of a configuration of points that, are invariant to changes in translation, rotation and scale.	
Superimposition	The transformation of one or more figures to achieve some geometric relationship to another	Allows the comparison of numerous specimens
Tangent space	Most relevant tangent space is a linear vector space that is tangent to Kendall's shape space are a point corresponding to the shape of a reference configuration	Due to being linear we are able to apply conventional statistical methods to study the variation on shape.
Thin plate spline T.P.S.	The form taken by a metal plate that is constrained at some combination of points and lines and otherwise free to adopt the form that minimizes bending energy	Provides a unique solution to the construction of D'Arcy Thompson type deformation grids from data in the form of two landmark configurations.
Type I land mark	Mathematical point whose claimed homology from case to case is supported by the strongest evidence.	
Type II land mark	Mathematical point whose claimed homology from case to case is supported only by geometric, not histological, evidence	
Type III landmark	Land mark having at least one deficient coordinate.	